



Activin-A impairs CD8 T cell-mediated immunity and immune checkpoint therapy response in melanoma

Katarina Pinjusic ¹, Olivier Andreas Dubey,¹ Olga Egorova,¹ Sina Nassiri,² Etienne Meylan,^{1,3} Julien Faget ^{1,4}, Daniel Beat Constam¹

To cite: Pinjusic K, Dubey OA, Egorova O, *et al.* Activin-A impairs CD8 T cell-mediated immunity and immune checkpoint therapy response in melanoma. *Journal for ImmunoTherapy of Cancer* 2022;**10**:e004533. doi:10.1136/jitc-2022-004533

► Additional supplemental material is published online only. To view, please visit the journal online (<http://dx.doi.org/10.1136/jitc-2022-004533>).

KP and OAD contributed equally.

KP and OAD are joint first authors.

Accepted 04 April 2022



© Author(s) (or their employer(s)) 2022. Re-use permitted under CC BY. Published by BMJ.

¹School of Life Sciences (SV), ISREC, Ecole Polytechnique Federale de Lausanne, Lausanne, Switzerland

²Bioinformatics Core Facility, Swiss Institute of Bioinformatics, Lausanne, Switzerland

³Laboratory of Immunology, Bordet Cancer Research Laboratories, Institut Jules Bordet, Faculty of Medicine, and Laboratory of Immunobiology, Faculty of Sciences, Université Libre de Bruxelles, Bruxelles, Belgium

⁴Equipe Immunity and Cancer ICM, INSERM U1194, Montpellier, France

Correspondence to

Professor Daniel Beat Constam; daniel.constam@epfl.ch

ABSTRACT

Background Activin-A, a transforming growth factor β family member, is secreted by many cancer types and is often associated with poor disease prognosis. Previous studies have shown that Activin-A expression can promote cancer progression and reduce the intratumoral frequency of cytotoxic T cells. However, the underlying mechanisms and the significance of Activin-A expression for cancer therapies are unclear.

Methods We analyzed the expression of the Activin-A encoding gene *INHBA* in melanoma patients and the influence of its gain- or loss-of-function on the immune infiltration and growth of *BRAF*-driven YUMM3.3 and iBIP2 mouse melanoma grafts and in B16 models.

Using antibody depletion strategies, we investigated the dependence of Activin-A tumor-promoting effect on different immune cells. Immune-regulatory effects of Activin-A were further characterized in vitro and by an adoptive transfer of T cells. Finally, we assessed *INHBA* expression in melanoma patients who received immune checkpoint therapy and tested whether it impairs the response in preclinical models.

Results We show that Activin-A secretion by melanoma cells inhibits adaptive antitumor immunity irrespective of *BRAF* status by inhibiting CD8⁺ T cell infiltration indirectly and even independently of CD4 T cells, at least in part by attenuating the production of CXCL9/10 by myeloid cells. In addition, we show that Activin-A/*INHBA* expression correlates with anti-PD1 therapy resistance in melanoma patients and impairs the response to dual anti-cytotoxic T-Lymphocyte associated protein 4/anti-PD1 treatment in preclinical models.

Conclusions Our findings suggest that strategies interfering with Activin-A induced immune-regulation offer new therapeutic opportunities to overcome CD8 T cell exclusion and immunotherapy resistance.

INTRODUCTION

Tumor immune surveillance by cytotoxic T lymphocytes (CTLs) and natural killer (NK) cells is frequently compromised by co-inhibitory receptors such as cytotoxic T-lymphocyte associated protein (CTLA-4) and programmed cell death 1 (PD1) that promote CTL exhaustion and immune self-tolerance.^{1,2} Thus, in cancers that are chronically inflamed by a high mutational

Key messages

⇒ Expression of the TGF β family member Activin-A encoded by the *INHBA* gene correlates with poor prognosis in many cancer types. Secretion of Activin-A by melanoma cells promotes tumor growth and correlates with reduced CD8⁺ T cell infiltration, but underlying mechanisms and their relevance for immunotherapies were unknown. This study shows that Activin-A indirectly dampens CD8⁺ T cells responses in melanoma, at least in part by directly impairing CXCL9 and CXCL10 secretion by myeloid cells in the tumor, leading to resistance to the immune checkpoint blockade therapy by combined anti-PD1/anti-cytotoxic T-Lymphocyte associated protein 4 treatment. These findings identify Activin-A as a promising new target to overcome immunotherapy resistance in melanoma and possibly other cancers.

burden, therapeutic anti-PD1 and anti-CTLA4 antibodies frequently reinvigorate antitumor immunity and drastically improve progression-free survival.³ In melanoma, therapy responsiveness also correlates with an IFN γ gene expression signature that includes antigen-presenting major histocompatibility complex (MHC) class I proteins.⁴ Conversely, low mutational burden, decreased antigen presentation, inhibition of CTL priming or infiltration, and their premature exhaustion all contribute to therapy resistance.⁵

Activins and Inhibins are gonadal hormones regulating the release of follicle-stimulating hormone. Inhibin antagonism of Activin-A signaling also protects against gonadal tumors and cancer-associated muscle wasting (cachexia).⁶ Activin-A encoded by the *INHBA* gene binds type II activin receptors (ACVR2) and activin receptor-like kinase 4 (ALK4, also known as ACVR1B) to activate SMAD2 and SMAD3 transcription factors. By contrast, receptor complexes containing ALK7 (ACVR1C) preferentially bind Activin-B and Activin-AB.⁷ While downregulation

of Activin receptor signaling within cancer cells increases their proliferation and tumor progression in pituitary, pancreas, esophagus, and colon,^{8–11} aberrant ALK4 signaling can promote cancer cell invasiveness, metastasis, and resistance to chemotherapy.^{12,13} *INHBA* mRNA is upregulated across diverse tumor types, including various skin malignancies,^{14,15} and elevated circulating Activin-A promotes cachexia and correlates with poor prognosis.¹⁶ However, whether Activin-A promotes or inhibits tumor progression depends on context.¹⁴ A dual role has been reported in melanoma, where ALK4 signaling in melanocytes inhibits proliferation and survival, whereas frequent gain of Activin-A secretion by melanoma cells promotes tumor growth and metastasis by inhibiting adaptive anti-tumor immunity.^{15,17} In addition, Activin-A increases tumor angiogenesis,¹⁵ possibly by enriching proangiogenic tumor-associated macrophages (TAMs) in the tumor microenvironment (TME), as demonstrated in skin squamous cell carcinoma.¹⁸ Activin-A is also secreted by macrophages themselves, at least in vitro.^{19–21} In addition, autocrine Activin-A signaling dampens proinflammatory cytokine and chemokine release by cultured blood monocytes and monocytic dendritic cells (DCs).^{22,23} Cultured CD4⁺ T cells express Activin-A after T cell receptor stimulation, specifically in Th2 and less in Th1 subsets.¹⁹ By contrast, Tregs can acquire *Alk7* expression and signaling during TGFβ-induced differentiation, and Activin-neutralizing antibodies were reported to reduce Treg frequency in syngeneic B16 melanoma grafts.²⁴ Here, we compare the impact of Activin-A on immune infiltrates in B16-F1 versus BRAF-driven mouse melanoma and test its effect on the response to immunotherapy. We show that melanoma cell-derived Activin-A indirectly inhibits CTL accumulation and proliferation, likely by interfering with the CXCL9/10-CXCR3 chemokine axis, and that its expression correlates with resistance to anti-PD1 therapy in melanoma patients and impairs the response to an anti-PD1/anti-CTLA4 combination in BRAF-driven mouse melanoma. Thus, inhibition of Activin-A emerges as a promising strategy to interfere with tumor-induced immune evasion and immunotherapy resistance.

MATERIALS AND METHODS

The complete experimental procedures and protocols are described in online supplemental material.

RESULTS

Activin-A secretion by melanoma cells decreases CTL and NK cell infiltration

Overexpression of Activin-A in B16-F1 mouse melanoma cells that do not transcribe endogenous *INHBA* can promote tumor immune evasion and metastatic growth in syngeneic hosts.¹⁵ To further validate this preclinical model, we first measured circulating Activin-A levels in the plasma of mice with B16-F1 mouse melanoma grafts expressing lentiviral *INHBA* (B16F1-βA) or empty vector

control (B16F1-Ctrl). Analysis by ELISA at the endpoint revealed that gain of *INHBA* expression increased the average plasma level of Activin-A from 0.9 to 34.7 ng/mL ($p=0.0015$, online supplemental figure S1A). By comparison, concentrations between 59 to 215 ng/mL have been reported in plasma of granulosa-cell-derived tumors in female Inhibin-deficient mice that secrete endogenous Activin-A.²⁵ As a first crude estimate of the net effect on proinflammatory and anti-inflammatory signals, we considered whether Activin-A altered the expression of specific effectors of tumor cell killing. Analysis of total RNA showed that *INHBA*-expressing tumors transcribed lower levels of *Gzmb*, *Prfn1*, and *Iilb* (online supplemental figure S1B–D), even though regulatory factors such as *Ii2* and *Ii10* were unchanged, at least at the mRNA level, and trends for decreased expression of *Ifng* and *Tnfa* mRNAs did not reach significance (online supplemental figure S1E–H). To survey the immune landscape of B16F1-βA and -Ctrl melanoma grafts in an unbiased manner, we analyzed tumor-infiltrating leucocytes (TILs) by flow cytometry using a 16-color antibody panel (online supplemental table S1). We observed a clear trend of Activin-A to diminish immune infiltrates that was associated with a significant reduction of CTL and NK cell proportions (figure 1A–C). Conversely, the proportion of conventional CD4 T cells increased, although without altering the abundance of CD4⁺ FoxP3⁺ regulatory T cells (figure 1D,E). Melanoma cell-derived Activin-A also enriched CD11b⁺ myeloid cells, CD11b⁺CD11c⁺F4/80⁺ DC, as well as CD11b⁺Ly6G^{hi} monocytes (figure 1F–H). By contrast, F4/80^{hi} TAMs that were highly abundant, and neutrophils gated as CD11b⁺Ly6G^{hi} immune population, and rare B cells did not change in frequency in B16F1-βA compared with control tumors (figure 1I,J and online supplemental figure S1I). To assess whether Activin-A influenced immune cell proliferation, we examined Ki67 expression. The fraction of proliferating CTLs decreased by 23% in B16F1-βA compared with B16F1-Ctrl tumors (online supplemental figure S1J). By contrast, no change was seen in the proliferation of tumor-infiltrating NK cells or Tregs, and the proliferation of FoxP3⁺ CD4⁺ T cells increased in βA-secreting tumors (online supplemental figure S1K–M). Together, these results show that Activin-A secretion by melanoma cells shifts the composition of tumor immune infiltrates from CTLs and NK cells toward increased non-regulatory CD4 T cells, DCs, and monocytes (online supplemental figure S1N).

Activin-A secretion by B16.OVA melanoma stimulates intratumoral antigen presentation

CTL activation and recruitment can be forestalled if cancer cells downregulate tumor antigen presentation by MHC class I molecules. To address whether Activin-A facilitates this process, we introduced control or *INHBA* lentivirus in B16.OVA mouse melanoma cell cells, a widely used B16-F0 subclone that has been engineered to present the ovalbumin (OVA) epitope SIINFEKL as a surrogate antigen. Flow cytometry of B16.OVA-βA and

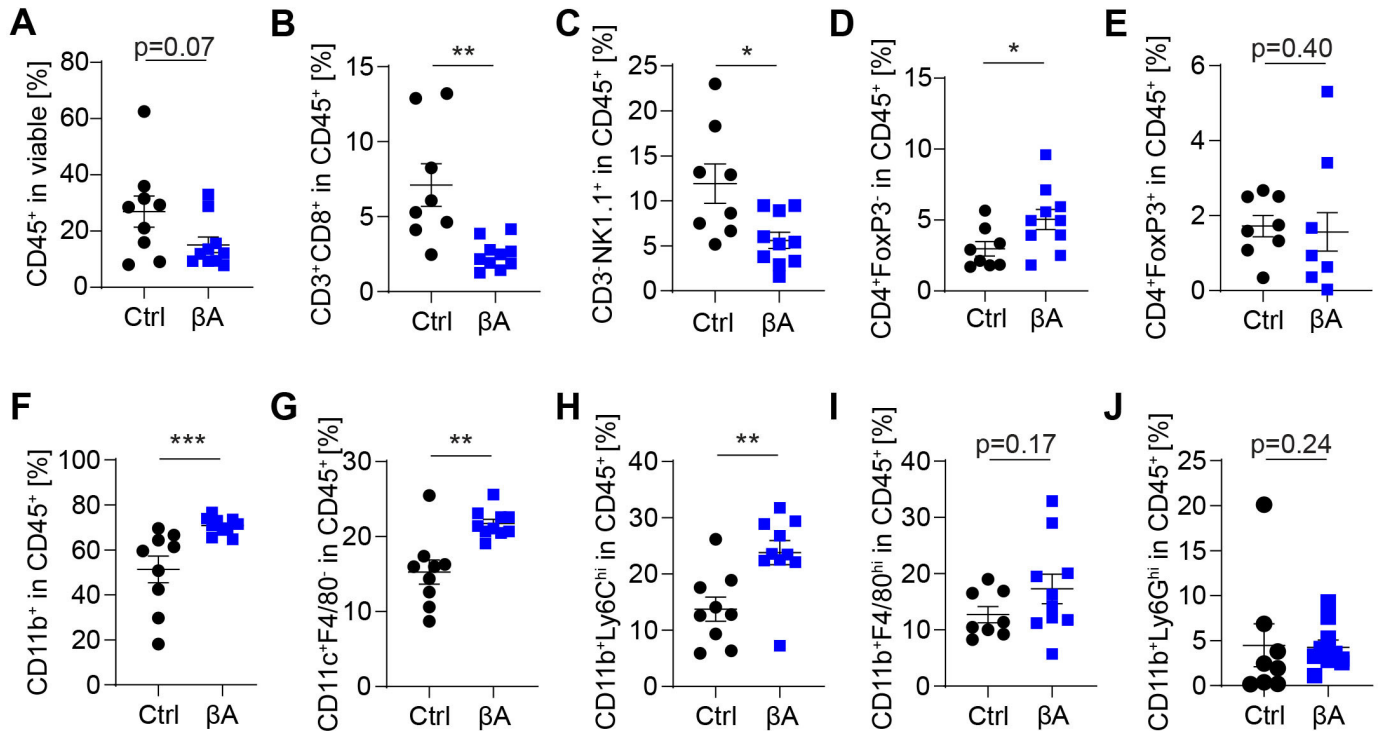


Figure 1 B16-F1 melanoma cell-derived Activin-A decreases tumor-infiltrating CTLs and NK cells. (A) Percentages of total CD45⁺ immune cells, and (B) CD3⁺CD8⁺ T cells, (C) CD3⁺NK1.1⁺ NK cells, (D) CD4⁺FoxP3⁺ T cells, (E) CD4⁺FoxP3⁺ Tregs, (F) CD11b⁺ myeloid cells, (G) CD11c⁺F4/80⁻ dendritic cells, (H) CD11b⁺Ly6C^{hi} monocytes, (I) CD11b⁺F4/80^{hi} TAMs, and (J) CD11b⁺Ly6G^{hi} neutrophils among CD45⁺ immune cells in syngeneic B16F1-Ctrl (n=8) and B16F1-βA (n=10) mouse melanoma grafts, quantified at the endpoint by flow cytometry. Data represent SEM, *p<0.05, **p<0.01, ***p<0.001, Student's t-test. CTLs, cytotoxic T lymphocytes; NK, natural killer.

-Ctrl cells treated with or without IFN γ revealed that cell surface H2Kb (MHC-I) and H2Kb-SIINFEKL complexes were not changed by transgenic *INHBA* (online supplemental figure S2A). Analogous results were obtained in B16F1-Ctrl and -βA cells that we transduced to express increased levels of OVA (online supplemental figure S2B). These results indicate that Activin-A does not interfere with IFN γ -inducible MHC-I loading. To address whether Activin-A inhibits MHC-I antigen cross-presentation, we analyzed intratumoral CD11c⁺ antigen-presenting cells (APCs) and their ability to cross-present OVA to CTLs in B16.OVA tumors (figure 2A). The frequency of intratumoral APCs was comparable in B16.OVA-βA and -Ctrl (figure 2B), and Activin-A increased H2Kb-SIINFEKL cell surface expression, rather than diminishing it (figure 2C). By contrast, the percentage of APCs, CD11c⁺CD8⁺ cells, and H2Kb-SIINFEKL⁺ subsets and their MHC-I expression in draining lymph nodes (dLNs) remained unchanged (online supplemental figure S2C–F). To test whether the enrichment of intratumoral APCs affects CTL priming, we stained the OVA-specific TCR of CD8⁺ T cells using SIINFEKL-specific MHC-I dextramer. Interestingly, OVA-specific CTLs were enriched 3-fold in βA compared with Ctrl tumors (figure 2D). Furthermore, while MHC-II expression on APCs was unchanged, their expression of co-stimulatory CD80 increased (figure 2E and F). These results suggest that Activin-A secretion by

B16 melanoma cells does not promote tumor growth by inhibiting antigen-specific CTL priming.

Activin-A inhibits CTLs independently of suppressive CD4⁺ T cells

To clarify how Activin-A promotes immune escape, we depleted CD8⁺ or CD4⁺ T cells in βA and Ctrl B16.OVA tumor-bearing mice. Selective cell depletion was confirmed in the blood and in tumors (online supplemental figure S2G,H). CD8⁺ T cell ablation with and without CD4⁺ T cell ablation further accelerated the growth of control tumors and neutralized the βA-induced growth advantage. By contrast, anti-CD4 treatment induced regression of B16.OVA-Ctrl tumors, but failed to slow the growth of B16.OVA-βA grafts (figure 2G). These data show that Activin-A overall inhibits tumor control by CTLs even independently of CD4⁺ T cells.

Activin-A does not directly inhibit CTL proliferation or cytotoxicity

To assess whether Activin-A can directly modulate CTL proliferation or function, splenocytes from OT-I mice expressing OVA-specific T cell receptor were stimulated with the OVA peptide SIINFEKL alone or together with Activin-A, and co-cultured thereafter with OVA-expressing melanoma cells (figure 3A). Real-time PCR analysis of total mRNA from treatment-naïve CD8⁺ cells of OT-I

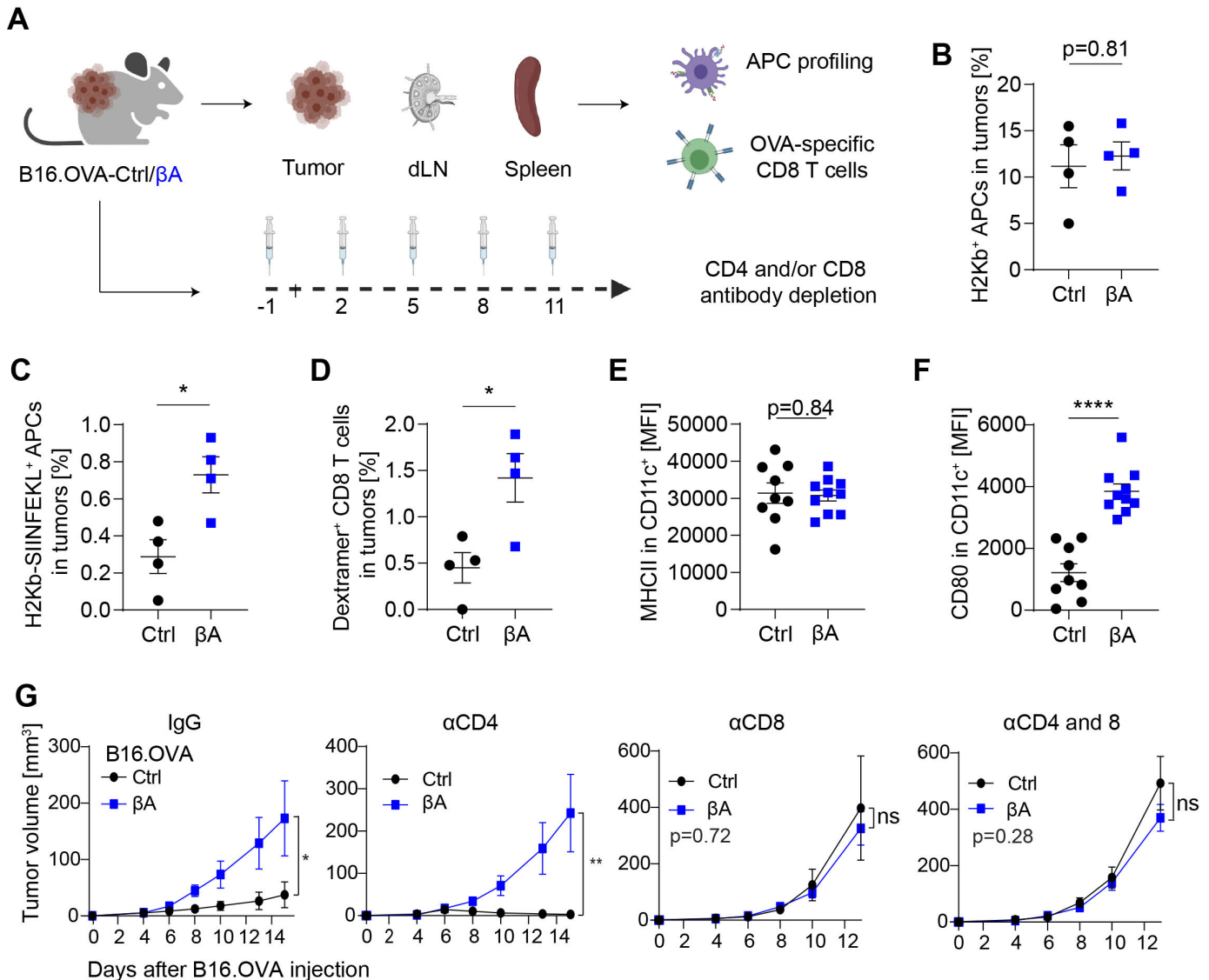


Figure 2 Activin-A accelerates melanoma growth by inhibiting antigen-specific CTLs, independently of CD4⁺ T cells and despite increased antigen cross-presentation. (A) Illustration of the workflow to assess the activation status and frequencies of antigen-presenting cells (APCs) and OVA-specific CD8⁺ T cells in tumors, draining lymph nodes (dLNs), and spleen of B16.OVA-Ctrl or B16.OVA-βA tumor-bearing mice (top), and the influence of anti-CD8 vs anti-CD4 depletion on tumor growth (bottom). (B) H2Kb surface expression and (C), H2Kb-SIINFEKL presentation by CD11c⁺ APCs in B16.OVA-Ctrl and B16.OVA-βA tumors analyzed by flow cytometry. (D) Dextramer-labeled H2Kb-SIINFEKL complexes on CD8⁺ T-cells from B16.OVA-Ctrl and B16.OVA-βA tumors. Error bars, SEM (n=4); *p<0.05, Student's t-test. (E) MHCII and (F) CD80 expression on tumor-infiltrating CD11c⁺ cells measured as mean fluorescence intensity (MFI) by flow cytometry (n = 8–10). Data represent SEM, ****p<0.0001, Student's t-test. (G) Growth curves of B16.OVA-Ctrl versus -βA in mice treated with IgG, αCD4, or αCD8 antibodies, or with a combination of αCD4 and αCD8. Error bars, SEM (n = 4–5 per group), *p<0.05, **p<0.01, Student's t-test. ns, not significant.

transgenic spleen, and from CD8 cell-depleted splenocytes revealed that both populations similarly transcribe *Acr2a*, *Acr2b*, and *Alk4*, but no *Alk7* (online supplemental figure S3A). However, treatment with Activin-A during 2 hours, or during OT-I cell activation for 4 days, or thereafter for 2 hours did not increase Smad2 phosphorylation, unlike control treatments with TGFβ (online supplemental figure S3B–D). Moreover, immunostaining of Ki67 and quantification of expanded OT-I cells revealed that SIINFEKL treatment stimulated the proliferation of splenocytes irrespective of Activin-A (figure 3B,C). Activin-A treatment also did not change the expression of the

activation markers CD25, CD69, or PD1, or the intracellular staining of TNFα, IFNγ, or Granzyme B (figure 3D, online supplemental figure S3E). These data and analogous treatments with up to 100 ng/mL show that CTLs withstand even high Activin-A dosage.²⁶ To assess whether Activin-A inhibits CTLs when it is secreted by melanoma cells, we cocultured activated OT-I T cells with melanoma cells. Since only 10%±5% of B16.OVA cells were killed by OT-I cells in vitro (online supplemental figure S3F), we used B16F1-Ctrl and B16F1-βA cells that we transduced with higher levels of OVA than those detected in B16.OVA cells (online supplemental figure S2B). Neither

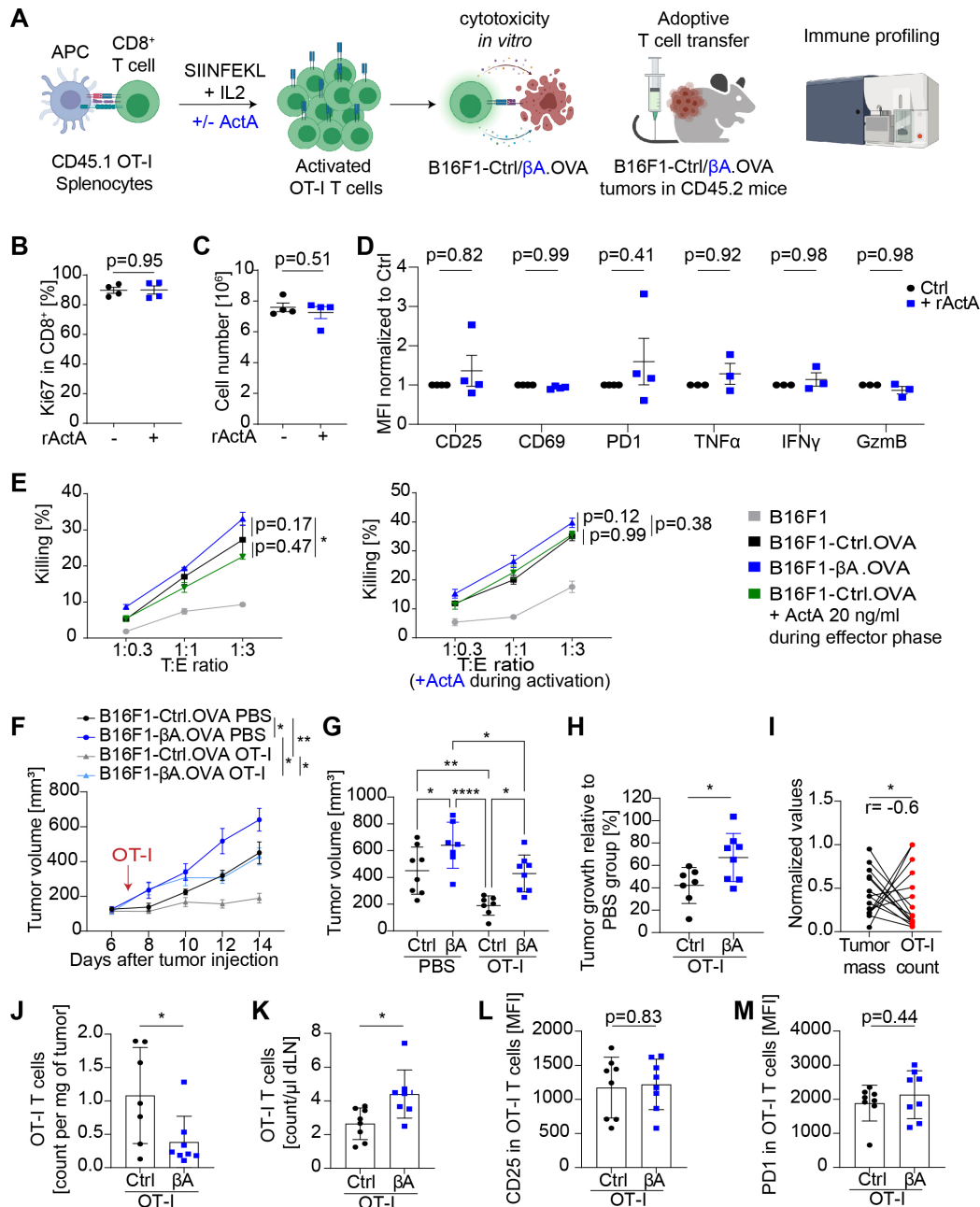


Figure 3 Activin-A diminishes the intratumoral accumulation but not the activation of in vitro-stimulated adoptive T cell grafts. (A) Strategy to compare the in vitro activation and cytotoxicity of CD8⁺ T cells in the presence and absence of melanoma cell-derived or exogenously added Activin-A. (B) Percentage of Ki67⁺ OT-I cells and (C) cell number count of expanded OT-I T cells after activation without or with Activin-A (n = 4 independent experiments). (D) Expression of CD25, CD69, and PD1 (n = 4 experiments) and TNFα, IFNγ, GranzymeB on OT-I T cells (n=3 experiments) after 4 days activation with or without Activin-A analyzed as mean fluorescence intensity normalized to the corresponding control of each flow cytometry experiment. Error bars, SEM; p values, two-way ANOVA with Tukey's correction for multiple comparison. (E) Tumor cell killing by OT-I cells activated in control conditions (left panel) or in presence of Activin-A (right panel) (n = 3-6 independent experiments). Error bars, SEM, p values, two-way ANOVA with Tukey's correction for multiple comparison. (F) Growth curves of B16F1-Ctrl.OVA and -βA.OVA tumors in syngeneic mice that received 1x10⁶ activated OT-I T cells or phosphate buffered saline (PBS) by i.v. injection, and (G), tumor volumes measured at the endpoint. (H) Reduction of B16F1-Ctrl.OVA and B16F1-βA.OVA tumor volumes by the OT-I transfer relative to average tumor volumes of the corresponding PBS-treated controls. Error bars, SEM (n = 7-8); p values, ordinary one-way ANOVA with Holm-Šidák correction for multiple comparisons. (I) Correlation of tumor mass with the number of OT-I TILs per mg of tumor. Tumor mass and OT-I count were normalized to the respective values of the largest tumor; n=15; r, two-tailed Pearson correlation analysis. (J) OT-I T cell count per mg of B16F1-Ctrl.OVA and B16F1-βA.OVA tumors and (K) per μl in their dLN suspension. Error bars, SEM (n = 7-8); p values, Student's t-test. (L, M) Mean fluorescence intensity of CD25 and PD1 protein staining in OT-I T cells analyzed by flow cytometry 1 week after the transfer into B16F1-Ctrl.OVA or B16F1-βA.OVA tumor-bearing mice. Error bars, SEM (n=7-8); *p<0.05, **p<0.01, ****p<0.0001, Student's t-test. ANOVA, analysis of variance; TILs, tumor-infiltrating leucocytes.

transgenic *INHBA* nor treatment with recombinant Activin-A before or after activation reduced CTL cytotoxicity (figure 3E). These results strongly suggest that melanoma-derived Activin-A inhibits CTLs indirectly.

Activin-A impairs tumor infiltration by adoptive T cell transfers

To distinguish whether Activin-A promotes CTL exclusion or exhaustion, we adoptively transferred activated CD45.1 OT-I T cells into CD45.2 tumor-bearing mice. OT-I T cell transfer, but not PBS control, halted the growth of B16F1-Ctrl.OVA tumors. By contrast, B16F1- β A.OVA tumors showed only a transient response to adoptive OT-I cell transfer (figure 3F–H). OT-I cell density inversely correlated with tumor size in all tumors analyzed; however, their overall number decreased 2.8-fold in β A tumors compared with Ctrl (figure 3I,J), even despite their increase in dLNs (figure 3K). Moreover, OT-I infiltration was accompanied by increased numbers of endogenous CTLs and other leucocytes specifically in B16F1-Ctrl.OVA tumors, suggesting increased inflammation compared with Activin-secreting tumors (online supplemental figure S3G–J). By contrast, OT-I cell activation marked by CD25, PD1, IFN γ , GzmB, and TNF α expression was similar in both groups (figure 3L and M, online supplemental figure S3K–M). These data show that Activin-A impairs intratumoral accumulation of CTLs even after their prior in vitro activation, consistent with an indirect inhibitory mechanism mediated by the TME.

Immune surveillance and tumor growth are regulated by *INHBA* in BRAF-driven melanoma

B16 mouse melanomas do not recapitulate common genetic mutations in human disease and are resistant to immunotherapies.²⁷ The most frequent melanoma driver mutations are oncogenic *BRAF*^{V600E} and loss of *CDKN2A* which are recapitulated in 2891L melanoma cells from *Tyr-CreERT2; Rosa26-lsl-rtTA; tetO-Braf*^{V600E}; *Cdkn2*^{-/-}; *Pten*^{-/-} iBIP2 mice,²⁸ and in YUMM3.3 cells from *Braf*^{V600E/+}; *Cdkn2a*^{-/-} mouse melanoma.²⁹ RT-qPCR and Western blot analyses revealed that both cell lines transcribe endogenous *Inhba* and accumulate Activin-A protein in the supernatant (SN) (online supplemental figure S4A,B). To monitor Activin-A signaling, we incubated the melanoma cell SNs on HepG2 reporter cells that were stably transduced with the SMAD3 luciferase reporter CAGA-Luc and with Renilla for signal normalization.³⁰ Treatment with iBIP2 2891L SN stimulated CAGA-Luc expression more than 100-fold, and this effect was blocked on addition of the Activin-A antagonist Follistatin (FST). By contrast, Activin-A present in YUMM3.3 SN failed to signal and even blocked CAGA-Luc induction by recombinant Activin-A and by iBIP2 2891 L conditioned medium (figure 4A), correlating with high mRNA expression levels of endogenous *Fst* (online supplemental figure S3C–E). To titrate out Fst and possibly other Activin-A antagonists, we transduced YUMM3.3 cells with *INHBA* lentivirus (YUMM3.3- β A) or empty vector (YUMM3.3-Ctrl).

Conversely, transduction of iBIP2 2891 L cells with Fc alone (iBIP2-Mock-Fc) or with the ligand trap AIIB-Fc (iBIP2-AIIB-Fc) served to mimic Activin-neutralizing factors and to test the role of endogenous Activin-A. As expected, the conditioned medium of YUMM3.3- β A induced CAGA-Luc more than 200-fold (figure 4A, B, C, top panel), whereas AIIB-Fc expression abrogated its induction by iBIP2 cell SN (figure 4A, bottom panel). Moreover, *INHBA* expression in YUMM3.3 cells accelerated tumor growth in syngeneic recipient mice, whereas expression of AIIB-Fc in iBIP2 2891L cells inhibited it (figure 4B), even though cell viability in culture was unchanged (online supplemental figure S4F).

To validate whether *INHBA*-induced tumor growth is mediated by the inhibition of adaptive antitumor immunity across multiple melanoma models, we transplanted tumor cells into immunodeficient *RagI*^{-/-} mice. YUMM3.3 and iBIP2 cells secreting functional Activin-A in *RagI*^{-/-} hosts grew indistinguishably from their respective Activin-depleted controls, confirming a critical role of adaptive immunity in *INHBA*-induced tumorigenesis (figure 4C). To assess how Activin-A remodels the TME in *Braf*^{V600E}-driven melanomas, we profiled TILs using 16-color flow cytometry. While Activin-A overexpression depleted CTLs in YUMM3.3 tumors, expression of ligand trap in iBIP2 2198L grafts increased it, and with no corresponding changes in CD4⁺ T cell frequencies (figure 4D,E). Moreover, in agreement with B16F1 tumor profiling, the frequency of FoxP3⁺CD4⁺ Treg cells was comparable in YUMM3.3- β A and -Ctrl tumors (figure 4F). Additionally, intracellular cytokine staining in YUMM3.3 tumor-infiltrating CTLs revealed a marked *INHBA*-induced decrease in IFN γ , TNF α , and GzmB protein levels (figure 4G–J). Collectively, these data demonstrate that Activin-A inhibits antitumor CTLs in both *BRAF* wild-type and mutant melanoma models, and without increasing the frequency of Tregs.

Activin-A inhibits CTLs independently of CSF1R⁺ TAMs

Analogous to B16F1 tumors, immune profiling revealed that the proportion of CD11b⁺ myeloid cells, but not Ly6C^{hi} monocytes, increased both in YUMM3.3 and iBIP2 β A-secreting tumors (online supplemental figure S5A,B). Specifically, *INHBA* expression increased the frequency of F4/80^{hi} macrophages in YUMM3.3, or CD11c⁺ F4/80⁺ DCs in iBIP2-Mock-Fc compared with AIIB-Fc, respectively (online supplemental figure S5C,D). To assess the contribution of TAMs to *INHBA*-driven tumor growth, we treated YUMM3.3 tumor-bearing mice with anti-mouse colony stimulating factor 1 receptor (CSF1R) antibodies or isotype controls. Administration of anti-CSF1R antibody failed to significantly alter tumor growth or change the CTL infiltration (online supplemental figure S5E,F), despite a pronounced decrease in the average frequency of tumor-infiltrating F4/80^{hi} TAMs by 61% in YUMM3.3-Ctrl, or by 86% in - β A tumors, respectively (online supplemental figure S5G). In good agreement, the expression of IFN γ and TNF α in CD8⁺ and CD4⁺ TILs

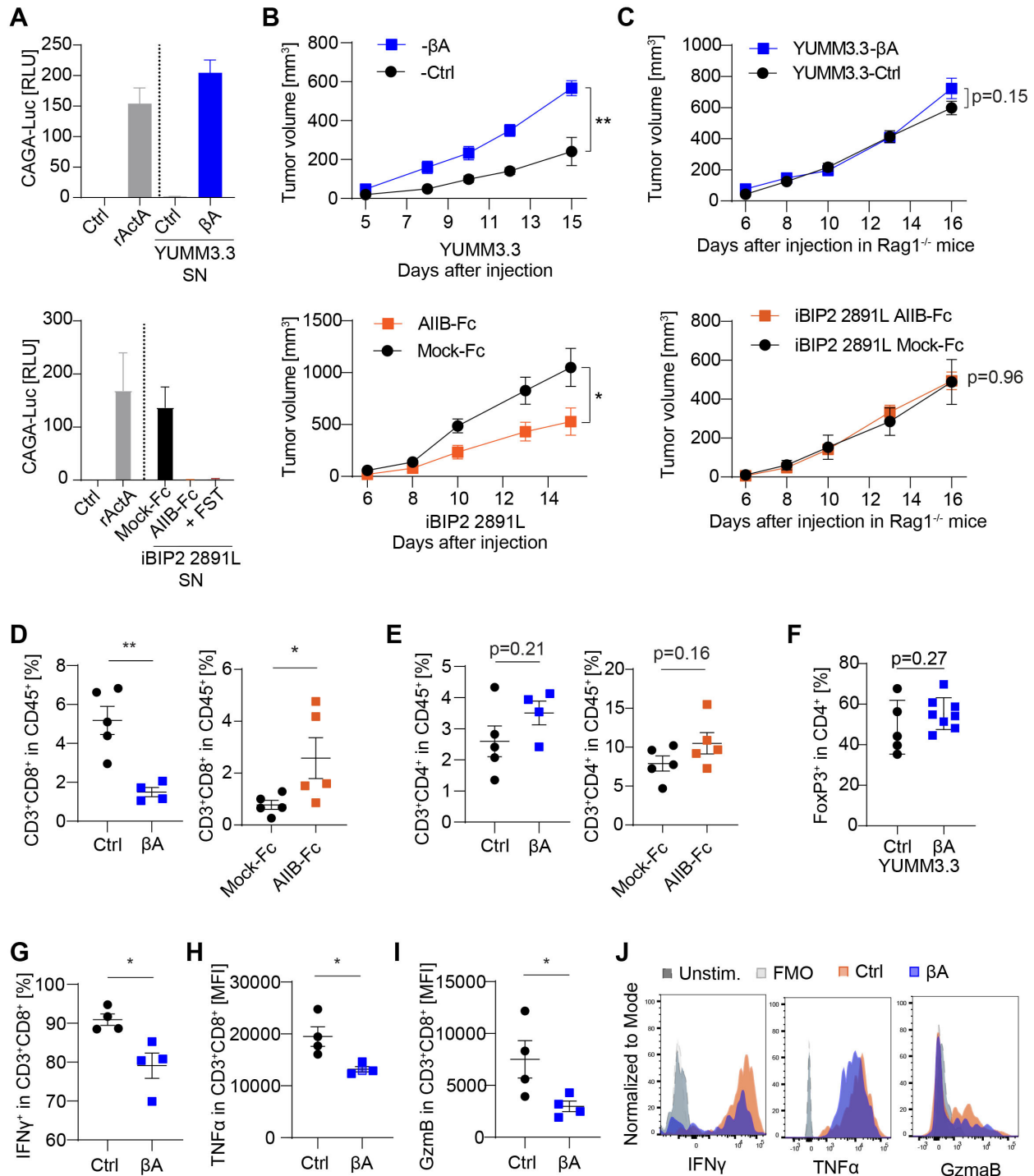


Figure 4 Activin-A accelerates the tumor growth and inhibits CTL accumulation and function also in BRAF-driven melanoma. (A) Induction of the CAGA-luc reporter of SMAD3 activity in HepG2 reporter cells after overnight incubation with conditioned media of YUMM3.3-Ctrl or β A stable cell lines (top), or of iBIP2 2891L Mock-Fc or AIIB-Fc cells (below). SN of parental iBIP2 2891L cells supplemented with or without 100 ng/ml FST are shown for comparison; n=2 independent experiments using triplicate samples. (B) Growth curves of YUMM3.3-Ctrl and β A tumors in syngeneic C57BL/6J female hosts (top), and of iBIP2 2891 L Mock-Fc or AIIB-Fc tumors in syngeneic FVB males (below) (n = 5 per group). (C) Growth curves of YUMM3.3-Ctrl and β A (top), and iBIP2 2891 L Mock-Fc and AIIB-Fc (below) tumor grafts in Rag1^{-/-} host (n=5 per group). (D, E) Flow cytometry of CD8⁺ or CD4⁺ T cell frequencies in YUMM3.3-Ctrl and β A (left), iBIP2 Mock-Fc and AIIB-Fc (right) tumor-infiltrating CD45⁺ cells (n=5). Error bars, SEM (n=5 per group); p value, Student's t-test. (F) Frequency of FoxP3⁺ cells among CD4⁺ TILs in YUMM3.3-Ctrl vs β A tumors. Error bars, SEM (n = 5 Ctrl and 8 β A tumors), Student's t-test. (G) IFN γ , (H) TNF α and (I) GzmB expression in CD8⁺ T cells from YUMM3.3-Ctrl and β A tumors at the endpoint. Error bars, SEM (n = 4-5); *p<0.05, **p<0.01, Student's t-test. (J) Representative histograms of intracellular IFN γ , TNF α , and Granzyme B flow cytometry analysis of CD8⁺ T-cells from YUMM3.3-Ctrl and β A syngeneic grafts after PMA/ionomycin stimulation. Stained unstimulated cells were used as fluorescence minus one (FMO) staining controls. CTLs, cytotoxic T lymphocytes; TILs, tumor-infiltrating leucocytes.

also remained unchanged (online supplemental figure S5H–K). These data suggest that F4/80^{hi} TAMs do not mediate *INHBA*-induced melanoma growth, or that they function redundantly with cells that are resistant to anti-CSF1R treatment.

Activin-A alters the immunoregulatory network in the TME

Since Activin-A failed to directly inhibit CTL functions *in vitro*, we sought to profile effects on relevant cytokines and chemokines in cultures of dissociated YUMM3.3-Ctrl and β A tumors (figure 5A). We found that compared with control, β A tumors increased the secretion of CXCL1, CCL11, CCL17, and CCL22, whereas CXCL9, CXCL10, and CXCL13 were decreased (figure 5B–H). Activin-A treatment also reduced CXCL9 and CXCL10 protein secretion by LPS-activated immortalized cDC1 cells in the absence but not in presence of the ALK4 inhibitor SB431542, and without altering cDC1 cell proliferation (online supplemental figure S6A–F). By contrast, the protein levels of secreted CCL2, CCL5, CXCL5, CCL3, CCL4, and CCL20 were comparable in YUMM3.3- β A and YUMM3.3-Ctrl tumors (online supplemental figure S7A–F). Dissociated β A tumors also secreted more IL4, which promotes Th2 responses and the polarization of suppressive macrophages, whereas IFN γ and IL10 secretion decreased compared with controls (figure 5I–K). By contrast, a tendency for increased IL5 and IL2 secretion did not reach significance, and levels of IL6, TNF α , IL9, IL21, IL13, IL22, IL17A, and IL17F were comparable between both groups (online supplemental figure S7G–P). Therefore, and since we observed no significant increase of *Tgfb1* mRNA expression (online supplemental figure S7Q) or of FoxP3⁺CD4⁺ Tregs in β A tumors, we wondered whether Activin-A stimulates tumor growth by promoting IL4 signaling. However, treatment with anti-IL4 antibody did not significantly slow the growth of YUMM3.3-Ctrl or β A tumors compared with isotype controls (online supplemental figure S7R). Thus, while melanoma cell-derived Activin-A supports myeloid cell infiltration at the expense of CTL recruitment to the tumor site, IL4 is dispensable for Activin-A-induced tumor growth advantage.

Secretion of CXCL9 and CXCL10 by myeloid cells is critical for CTL recruitment and tumor control after adoptive T cell transfer or ICB treatment.^{31–33} Absolute quantification of F4/80⁺ monocytic macrophage (MoMac) or DCs showed no change in YUMM3.3- β A compared with YUMM3.3-Ctrl tumors, and proportions of MoMac subtypes were comparable between the two groups (figure 5L and M). However, in both MHCI-1⁺CD11c⁺ and F4/80^{hi} MoMac, and CCR7⁺ DC3 cells, *INHBA*-expressing tumors showed significantly reduced intracellular staining of CXCL9 (figure 5N, online supplemental figure S7S). Together, these data indicate that Activin-A expression in tumor interferes with CTL recruitment by attenuating the expression of CXCL9 in MoMac and DCs.

INHBA expression in melanoma augments their resistance to ICB immunotherapy

Analysis of public datasets revealed that *INHBA* mRNA expression in human melanoma only weakly correlates with survival¹⁵ or metastatic burden (online supplemental figure S8A). Average *INHBA* mRNA levels in the TCGA dataset of human melanoma (SKCM) were also comparable in primary and metastatic tumors (online supplemental figure S8B). Interestingly, however, in a published dataset on genomic and transcriptomic changes from 28 melanoma patients treated with anti-PD1, immunotherapy resistance strongly correlated with *INHBA* expression (figure 6A).³⁴ Innate resistance to immunotherapies by anti-PD1, anti-CTLA4, or anti-CSF1R antibodies is also seen in iBIP2 mouse melanoma.²⁸ To test whether resistance involves endogenous Activin-A, we administered anti-PD1/anti-CTLA4 immune checkpoint blockade (ICB) therapy to iBIP2-AIIB-Fc or iBIP2-Mock-Fc tumor-bearing mice. While ICB administration failed to significantly inhibit iBIP2-Mock-Fc tumor growth, it led to uniform regression of AIIB-Fc tumors (figure 6B). FACS analysis of TILs revealed that this response to ICB was accompanied by increased CTL infiltration and by a higher frequency of CD8⁺ and CD4⁺ T cells expressing IFN γ (figure 6C–E). To test whether *INHBA* is both necessary and sufficient to confer ICB resistance, we administered anti-PD1/anti-CTLA4 ICB therapy or IgG control antibodies to YUMM3.3-Ctrl and β A tumor grafts. As expected, YUMM3.3-Ctrl tumors invariably responded to ICB therapy, with 64% of the tumors achieving complete regression (n=7/11) and 36% partial response (n=4/11). By contrast, a majority of YUMM3.3- β A tumor-bearing mice showed progressive disease (n=5/12, 42%) or only a partial response (n=2/12, 17%) despite ICB treatment (figure 6F–H, online supplemental figure S8C). Together, these results demonstrate that *INHBA*-induced changes in the TME impair the response of melanoma to ICB therapy.

DISCUSSION

Here, we found that Activin-A indirectly inhibits CTL proliferation and accumulation in *BRAF* wild-type and oncogenic mutant preclinical melanoma models and that its expression correlates with anti-PD1 therapy resistance in human melanoma and impairs the response to combined anti-PD1/anti-CTLA4 therapy in gain-of-function and loss-of-function settings. Immune-profiling and cell depletion experiments revealed that melanoma cell-derived Activin-A reduces the dependence on suppressive CD4⁺ T cells to escape immune surveillance, correlating with the diminished secretion of specific chemokines such as CXCL9 and CXCL10. Our findings suggest that Activin-A neutralization is a promising strategy to sensitize *INHBA*-expressing tumors to ICB therapy.

In all melanoma models examined, and irrespective of their *BRAF* status, *INHBA* expression reduced the

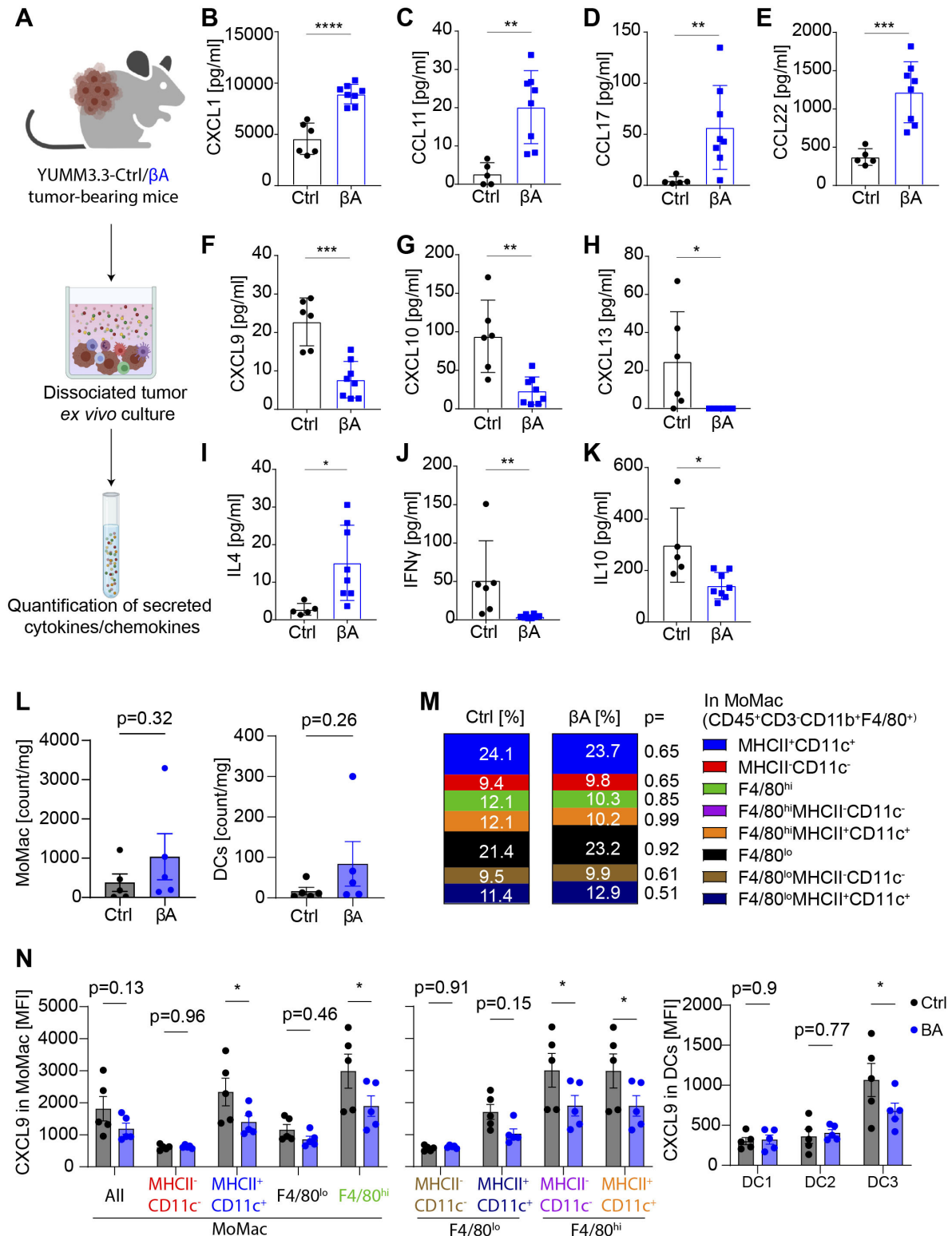


Figure 5 Activin-A alters the immunoregulatory network in the TME. (A) Illustration of the experimental procedure: YUMM3.3-Ctrl and β A tumors were dissected, cell numbers were normalized and cultured ex vivo. Secreted chemokines and cytokines in the culture supernatant were quantified. (B–K) Secretion of CXCL1, CCL11, CCL17, CCL22, CXCL9, CXCL10, CXCL13, IL4, IFN γ , and IL10 by dissociated YUMM3.3-CTRL and YUMM3.3- β A tumor cells during 24 hours of ex vivo culture. Error bars, SEM (n = 5–6 Ctrl and 8- β A tumors). *P<0.05, **p<0.01, ***p<0.001, ****p<0.0001, Mann-Whitney U test for non-parametric data and a two-tailed t-test for parametric data. (L) Quantification of MoMac (CD45⁺CD3⁺CD11b⁺F4/80⁺) and DC (CD45⁺CD3⁺F4/80⁺MHCII⁺CD11c⁺) infiltration and (M) proportions of MoMac subsets in YUMM3.3-Ctrl versus β A tumors (n = 5). (N) CXCL9 production measured as MFI in MoMac and DC subpopulations: XCR1⁺ DC1, CD172a⁺ DC2, CCR7⁺ DC3. Error bars, SEM (n=5 tumors per group). *P<0.05, two-tailed t-test. DC, dendritic cell; MFI, mean fluorescence intensity; MHC, major histocompatibility complex; TME, tumor microenvironment.

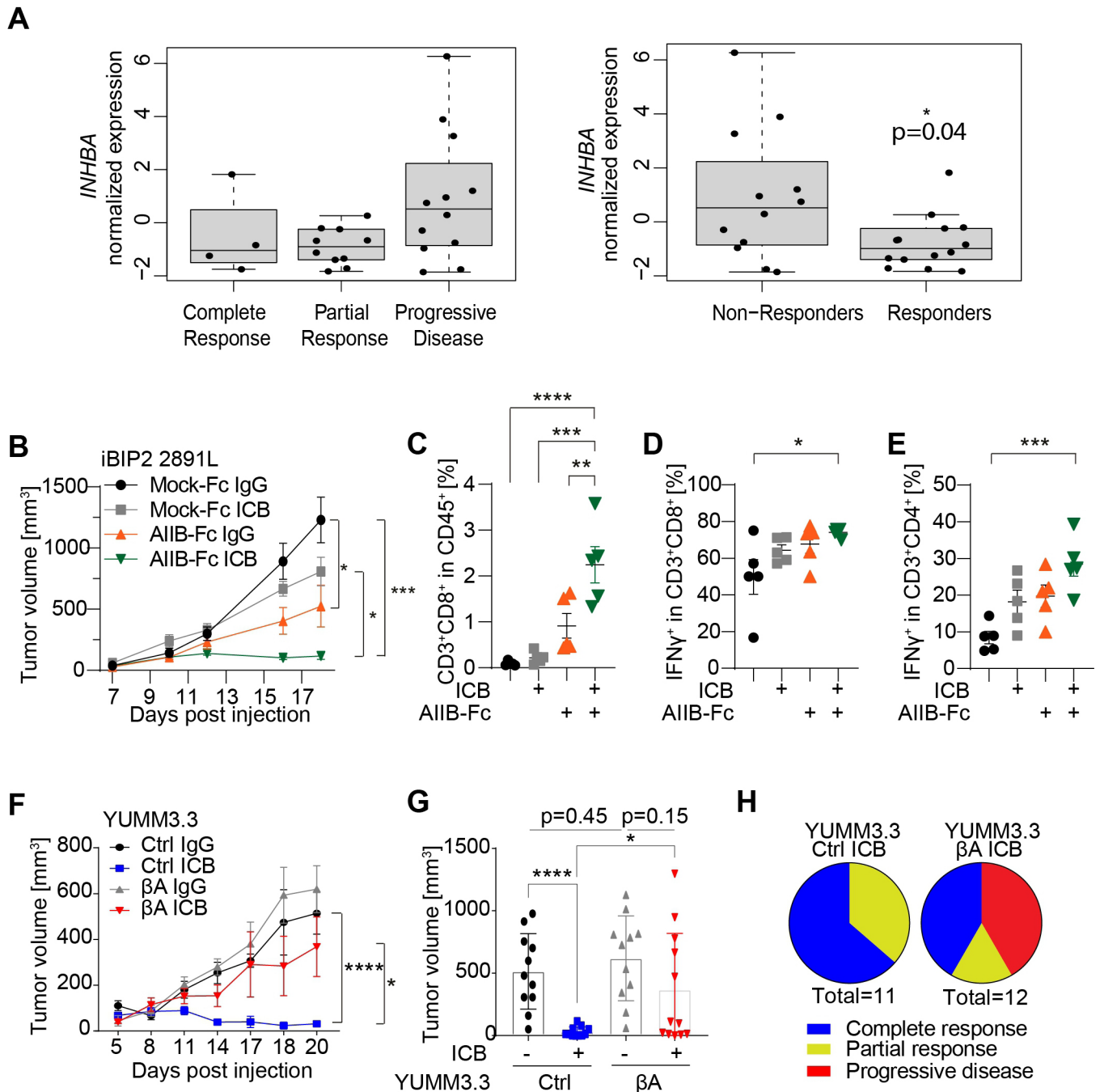


Figure 6 *INHBA* expression in melanoma promotes resistance to ICB immunotherapy. (A) Relative expression levels of *INHBA* mRNA in biopsies of 26 pretreatment melanoma patients grouped by the course of disease after receiving anti-PD1 therapy (left; one-way ANOVA not significant), or as responders ($n=14$) or non-responders ($n=12$), $p=0.04$, Welch two sample t-test (2) based on irRECIST criteria (3). (B) Growth curves of iBIP2 2891L Mock-Fc and iBIP2 2891L AIB-Fc tumor grafts in FVB/N mice after treatment with α PD-1 and α CTLA4 (ICB), or with IgG control antibodies. (C–E) Relative frequencies of (C) total and (D) IFN γ^+ CD8 $^+$ T cells, and of (E) IFN γ^+ CD4 $^+$ T cells in iBIP2 2891L Mock-Fc vs AIB-Fc tumors treated with ICB or control IgG antibodies. Error bars, SEM ($n=5$ per genotype); ** $p<0.01$, *** $p<0.001$, **** $p<0.0001$, ordinary one-way ANOVA with Holm-Šidák correction for multiple comparisons. (F) Growth curves and (G), volumes of YUMM3.3-CTRL and $-\beta$ A tumors treated with IgG or ICB antibodies. (H) Pie charts of the response to anti-PD1/anti-CTLA4 ICB therapy in YUMM3.3-CTRL and YUMM3.3- β A tumors. Error bars, SEM ($n=11-12$); * $P<0.05$, ** $p<0.01$, *** $p<0.001$, **** $p<0.0001$, two-tailed Student's t-test. ANOVA, analysis of variance.

frequency of intratumoral CTLs and NK cells. Activin-A can attenuate NK cell proliferation and cytotoxicity directly, although modestly.^{26 35} In addition, NK cells are likely depleted due to impaired accumulation of

CTLs.^{36 37} Indeed, several lines of evidence suggest that immune evasion induced by Activin-A requires reprogramming of the TME, which in turn primarily inhibits the recruitment and activity of CTLs: First, the tumor

growth advantage mediated by Activin-A was lost in *Rag1*^{-/-} hosts that specifically lack adaptive immunity. Second, Activin-A secretion by melanoma cells stimulated T cell priming rather than inhibiting it, and only locally within the TME, even though it accumulates in the circulation and induces systemic muscle wasting. Third, Activin-A diminished tumor infiltration of in vitro-activated OVA-specific adoptive T cell grafts, and despite the fact that they maintained the expression of activation markers and of cytotoxic effector molecules for at least 1 week after adoptive transfer into tumor-bearing mice. By contrast, Activin-A treatment of OVA-specific T cells in vitro altered neither their proliferation nor their cytotoxicity. Accordingly, Activin-A also failed to stimulate Smad2 phosphorylation in activated CD8⁺ T cells and in naïve splenocytes expressing *Acrv2* and *Alk4* mRNAs. Possible inhibitory mechanisms include the expression of specific antagonists or post-transcriptional regulation of Activin receptors. Our finding that Activin-A only indirectly inhibited CD8⁺ T cell proliferation agrees with earlier reports that it does not alter the proliferation of CD8⁺ T cells or their IFN γ expression, or that it may do so only indirectly.^{23,38} Lastly, analysis in B16.OVA melanoma revealed that depletion of CD8⁺ T cells abolishes the tumor-promoting activity of *INHBA*. By contrast, anti-CD4 depletion only diminished the growth of B16.OVA-Ctrl but not of β A tumors. Thus, Activin-A reduces the dependence of these tumors on suppressive CD4⁺ T cells to escape immune detection, rather than increasing it. Lack of Tregs in *Cd4*^{-/-} hosts also does not slow *INHBA*-driven growth of a papilloma virus-induced skin cancer model.¹⁸ At first glance, this is surprising since Activin-A can synergize with TGF β to induce Tregs.^{39,40} However, Tregs only express *Alk7*, which preferably binds *INHBB*-derived Activins.²⁴ The failure of melanoma cell-derived Activin-A to enrich Tregs or to increase CD4⁺ T cell-mediated immune evasion in any of our preclinical models points to its limited bioavailability in this cell type.

Cancer cells can evade CTLs by reducing tumor antigen presentation, and inefficient MHC-I induction by IFN γ in melanoma correlates with resistance to ICB therapy.⁴ Our analysis revealed that *INHBA* expression attenuated the levels of IFN γ protein in bulk tumors and in infiltrating CTLs, yet without altering MHC-I expression by tumor cells. Another pillar of antitumor T cell response involves the cross-presentation of tumor antigens by DCs. Treatment with Activin-A can inhibit or promote CD8⁺ T cell activation by in vitro-differentiated mouse and human DCs, depending on the context.^{23,41} Our analysis revealed that the majority of intratumoral APCs are CD11b⁺ myeloid cells. Activin-A increased their antigen presentation rather than inhibiting it, and without altering their overall frequency or their migration to dLNs, or their MHC-I or -II expression. Such efficient cross-presentation even despite the presence of Activin-A sharply contrasts the potent inhibition of DCs by Activin-induced Tregs in allergic airway disease,⁴² consistent with our finding that melanoma cell-derived Activin-A did not enrich Tregs.

Furthermore, instead of activating CTLs, the stimulation of cross-presenting APCs by Activin-A associated with reduced CTL proliferation and effector functions. Thus, besides inhibiting CTL recruitment, Activin-A reprograms the TME to interfere with their proper activation.

In all melanoma models examined, the depletion of lymphocytes by Activin-A was accompanied by a proportionate increase in myeloid infiltrate, but its composition varied considerably. In B16-F1 melanoma, Activin-A promoted the recruitment of Ly6C^{hi} monocytes without further enriching TAMs. By contrast, in iBIP2 and YUMM3.3 grafts, it mainly enriched TAMs, but not monocytes. Whether such differences in the composition of myeloid infiltrates and their relative enrichment by Activin-A depend on BRAF status or other tumor-specific driver mutations is unknown. However, macrophages are also enriched by a keratinocyte-specific *INHBA* transgene in HPV8-induced skin tumors, and their depletion by anti-CSF1R treatment delayed the onset of tumor formation.¹⁸ By contrast, we found that depletion of CSF1R⁺ TAMs did not reduce *INHBA*-induced melanoma growth. In good agreement, CSF1R antibody depletion also failed to slow tumor growth in iBIP2 transgenic mice or in mice receiving Yummer1.7 melanoma cell transplants.²⁸ Myeloid-derived suppressive cells can also be recruited by the chemokine receptor CCR2 that is induced by Activin-A in monocyte-derived macrophages.⁴³ Interestingly, CCR2 inhibition can boost ICB therapies in preclinical models of several cancer types.⁴⁴ However, analysis in B16-F10 melanoma-bearing mice revealed that CCR2 inhibition depleted only a prometastatic subpopulation of lung-resident macrophages without diminishing primary tumor growth.⁴⁴ Similarly, genetic ablation of CCR2⁺ monocytes also afforded no protection against *INHBA*-driven skin tumors or against their infiltration by tumor-promoting TAMs.¹⁸

Tumor control after adoptive T cell transfer and the response of melanoma to immune checkpoint therapy depend on the IFN γ -inducible chemokines CXCL9/10 to recruit CXCR3-expressing T cells to the tumor bed.^{32,45,46} CXCL9 and CXCL10 expression also correlate with T cell infiltration and survival in stage-III melanoma patients.^{47–49} However, little is known about negative regulators of CXCL9/10 expression in cancer. Our chemokine profiling of dissociated YUMM3.3 tumors revealed that Activin-A expression diminished IFN γ and CXCL9/10 secretion. In vivo validation of CXCL9 expression confirmed its downregulation both in CCR7⁺ DCs and in MHCII⁺CD11c⁺ MoMac and F4/80hi TAMs. Activin-A treatment of a widely used mouse cDC1 cell line during activation by LPS and IFN γ within 24 hours led to a significant decrease in CXCL9 and CXCL10 secretion. Conversely, treatment of monocyte-derived DCs with FST has previously been shown to rapidly increase CXCL10 secretion, indicating direct inhibition also by autocrine Activin signaling.²³ TAMs expressing CSF1R are not essential to mediate T cell exclusion by Activin-A, since their depletion did not slow *INHBA*-dependent

tumor growth. However, alternative CXCL9/10 sources including CSF1R-independent MoMac populations and DCs are critical for CTL recruitment.³² In addition, Activin-A increased the levels of secreted CCL11, CCL17, CCL22, and IL4. CCL11 expression is induced by hypoxia in breast cancer cells to recruit CCR5⁺ macrophages,⁵⁰ whereas CCL17 and CCL22 secreted by tumor cells, TAMs, and/or DCs can attract CCR4-expressing CD4⁺ Th17, Treg, and Th2 cells and monocytes with protumor or antitumor activities.⁵¹ Activin-A secretion by melanoma cells clearly stimulated tumor growth independently of CD4⁺ cells and IL-4. However, the potential roles of DCs and of monocyte recruitment by CCR4 ligands warrant further investigation.

Our analysis of a publicly available dataset indicated that *INHBA* was upregulated in melanoma patients with progressive disease after anti-PD1 therapy.³⁴ Furthermore, neutralization of endogenous Activin-A by a soluble form of ACVRIIB sensitized iBIP2 melanoma grafts to combined anti-PD1/anti-CTLA4 blockade, whereas *INHBA* gain-of-function in YUMM3.3 melanoma grafts inhibited the response. In both settings and across different models, ICB response correlated with CTL infiltration and activation as assessed by intracellular IFN γ staining. These results strongly support a clinically relevant function for Activin-A signaling in the resistance to checkpoint inhibitors in melanoma.

Twitter Katarina Pinjusic @K_Pinjusic

Acknowledgements The authors thank Drs Anna C. Obenaus (Vienna, Austria) and Martin McMahon (San Francisco, USA) for providing YUMM3.3 cells, Drs Douglas Hanahan and Daniel Speiser (Lausanne, Switzerland) for iBIP2 2891L cell lines and for the protocol to culture splenocytes, respectively, and Dr Michele De Palma and members of the Constan lab for comments on the manuscript.

Contributors Conceptualization, OAD, KP and DBC; methodology, OAD, KP, SN, JF and DBC; bioinformatics analysis, SN; validation, KP, OAD, OE; formal analysis, KP, OAD, SN; investigation, KP, OAD, OE; resources, SN, JF, EM; data curation, SN; writing—original Draft, KP, DBC; review and editing, KP, OAD, JF, EM, DBC; visualization, KP, OAD, SN; supervision, project administration, funding acquisition, and guarantor, DBC.

Funding This work was supported by grants 31003A_179330 of the Swiss National Science foundation and KFS-4454-02-2018 from the Swiss Cancer League and by the Anna Fuller Fund award 20495 to DBC, and by services of the Center of PhenoGenomics and Flow Cytometry Research Core Facilities at the School of Life Sciences of EPFL.

Competing interests None declared.

Patient consent for publication Not applicable.

Provenance and peer review Not commissioned; externally peer reviewed.

Data availability statement Data sharing not applicable as no datasets generated and/or analysed for this study.

Supplemental material This content has been supplied by the author(s). It has not been vetted by BMJ Publishing Group Limited (BMJ) and may not have been peer-reviewed. Any opinions or recommendations discussed are solely those of the author(s) and are not endorsed by BMJ. BMJ disclaims all liability and responsibility arising from any reliance placed on the content. Where the content includes any translated material, BMJ does not warrant the accuracy and reliability of the translations (including but not limited to local regulations, clinical guidelines, terminology, drug names and drug dosages), and is not responsible for any error and/or omissions arising from translation and adaptation or otherwise.

Open access This is an open access article distributed in accordance with the Creative Commons Attribution 4.0 Unported (CC BY 4.0) license, which permits

others to copy, redistribute, remix, transform and build upon this work for any purpose, provided the original work is properly cited, a link to the licence is given, and indication of whether changes were made. See <https://creativecommons.org/licenses/by/4.0/>.

ORCID iDs

Katarina Pinjusic <http://orcid.org/0000-0002-5070-3340>

Julien Faget <http://orcid.org/0000-0003-0848-7135>

REFERENCES

- Mahmoud F, Shields B, Makhoul I, *et al*. Immune surveillance in melanoma: from immune attack to melanoma escape and even counterattack. *Cancer Biol Ther* 2017;18:451–69.
- Fife BT, Bluestone JA. Control of peripheral T-cell tolerance and autoimmunity via the CTLA-4 and PD-1 pathways. *Immunity* 2008;28:166–82.
- Larkin J, Chiarion-Sileni V, Gonzalez R, *et al*. Five-year survival with combined nivolumab and ipilimumab in advanced melanoma. *N Engl J Med* 2019;381:1535–46.
- Grasso CS, Tsoi J, Onyshchenko M, *et al*. Conserved interferon- γ signaling drives clinical response to immune checkpoint blockade therapy in melanoma. *Cancer Cell* 2020;38:500–15.
- Kalbasi A, Ribas A. Tumour-intrinsic resistance to immune checkpoint blockade. *Nat Rev Immunol* 2020;20:25–39.
- Bloise E, Ciarmela P, Dela Cruz C, *et al*. Activin A in mammalian physiology. *Physiol Rev* 2019;99:739–80.
- Tsuchida K, Nakatani M, Yamakawa N, *et al*. Activin isoforms signal through type I receptor serine/threonine kinase ALK7. *Mol Cell Endocrinol* 2004;220:59–65.
- Loomans HA, Arnold SA, Hebron K, *et al*. Loss of ACVR1B leads to increased squamous cell carcinoma aggressiveness through alterations in cell-cell and cell-matrix adhesion proteins. *Am J Cancer Res* 2017;7:2422–37.
- Su GH, Bansal R, Murphy KM, *et al*. ACVR1B (ALK4, activin receptor type 1B) gene mutations in pancreatic carcinoma. *Proc Natl Acad Sci U S A* 2001;98:3254–7.
- Takeda H, Kataoka S, Nakayama M, *et al*. CRISPR-Cas9-mediated gene knockout in intestinal tumor organoids provides functional validation for colorectal cancer driver genes. *Proc Natl Acad Sci U S A* 2019;116:15635–44.
- Danila DC, Zhang X, Zhou Y, *et al*. Overexpression of wild-type activin receptor Alk4-1 restores activin antiproliferative effects in human pituitary tumor cells. *J Clin Endocrinol Metab* 2002;87:4741–6.
- Marini KD, Croucher DR, McCloy RA, *et al*. Inhibition of activin signaling in lung adenocarcinoma increases the therapeutic index of platinum chemotherapy. *Sci Transl Med* 2018;10:eaat3504.
- Chen L, De Menna M, Groenewoud A, *et al*. A NF- κ B-Activin a signaling axis enhances prostate cancer metastasis. *Oncogene* 2020;39:1634–51.
- Ries A, Schelch K, Falch D, *et al*. Activin A: an emerging target for improving cancer treatment? *Expert Opin Ther Targets* 2020;24:985–96.
- Donovan P, Dubey OA, Kallioinen S, *et al*. Paracrine activin-A signaling promotes melanoma growth and metastasis through immune evasion. *J Invest Dermatol* 2017;137:2578–87.
- Hulmi JJ, Nissinen TA, Penna F, *et al*. Targeting the activin receptor signaling to counteract the Multi-Systemic complications of cancer and its treatments. *Cells* 2021;10:516.
- Murakami M, Suzuki M, Nishino Y, *et al*. Regulatory expression of genes related to metastasis by TGF- β and activin A in B16 murine melanoma cells. *Mol Biol Rep* 2010;37:1279–86.
- Antsiferova M, Piwko-Czuchra A, Cangkrama M, *et al*. Activin promotes skin carcinogenesis by attraction and reprogramming of macrophages. *EMBO Mol Med* 2017;9:27–45.
- Ogawa K, Funaba M, Chen Y, *et al*. Activin A functions as a Th2 cytokine in the promotion of the alternative activation of macrophages. *J Immunol* 2006;177:6787–94.
- Sierra-Filardi E, Puig-Kröger A, Blanco FJ, *et al*. Activin a skews macrophage polarization by promoting a proinflammatory phenotype and inhibiting the acquisition of anti-inflammatory macrophage markers. *Blood* 2011;117:5092–101.
- Li N, Cui X, Ge J, *et al*. Activin A inhibits activities of lipopolysaccharide-activated macrophages via TLR4, not of TLR2. *Biochem Biophys Res Commun* 2013;435:222–8.
- González-Domínguez Érika, Domínguez-Soto Ángeles, Nieto C, *et al*. Atypical activin A and IL-10 production impairs human CD16+

- monocyte differentiation into anti-inflammatory macrophages. *J Immunol* 2016;196:1327–37.
- 23 Robson NC, Phillips DJ, McAlpine T, *et al.* Activin-A: a novel dendritic cell-derived cytokine that potently attenuates CD40 ligand-specific cytokine and chemokine production. *Blood* 2008;111:2733–43.
- 24 Ni X, Tao J, Barbi J, *et al.* YAP is essential for treg-mediated suppression of antitumor immunity. *Cancer Discov* 2018;8:1026–43.
- 25 Matzuk MM, Finegold MJ, Mather JP, *et al.* Development of cancer cachexia-like syndrome and adrenal tumors in inhibin-deficient mice. *Proc Natl Acad Sci U S A* 1994;91:8817–21.
- 26 Robson NC, Wei H, McAlpine T, *et al.* Activin-A attenuates several human natural killer cell functions. *Blood* 2009;113:3218–25.
- 27 Kuczynski EA, Krueger J, Chow A, *et al.* Impact of chemical-induced mutational load increase on immune checkpoint therapy in poorly responsive murine tumors. *Mol Cancer Ther* 2018;17:869–82.
- 28 Neubert NJ, Schmittnaegel M, Bordry N, *et al.* T cell-induced CSF1 promotes melanoma resistance to PD1 blockade. *Sci Transl Med* 2018;10:eaan3311.
- 29 Meeth K, Wang JX, Micevic G, *et al.* The YUMM lines: a series of congenic mouse melanoma cell lines with defined genetic alterations. *Pigment Cell Melanoma Res* 2016;29:590–7.
- 30 Fuerer C, Nostro MC, Constam DB. Nodal Gdf1 heterodimers with bound prodomains enable serum-independent nodal signaling and endoderm differentiation. *J Biol Chem* 2014;289:17854–71.
- 31 Zilionis R, Engblom C, Pfirschke C, *et al.* Single-cell transcriptomics of human and mouse lung cancers reveals conserved myeloid populations across individuals and species. *Immunity* 2019;50:1317–34.
- 32 Spranger S, Dai D, Horton B, *et al.* Tumor-residing Batf3 dendritic cells are required for effector T cell trafficking and adoptive T cell therapy. *Cancer Cell* 2017;31:711–23.
- 33 House IG, Savas P, Lai J, *et al.* Macrophage-derived CXCL9 and CXCL10 are required for antitumor immune responses following immune checkpoint blockade. *Clin Cancer Res* 2020;26:487–504.
- 34 Hugo W, Zaretsky JM, Sun L, *et al.* Genomic and transcriptomic features of response to anti-PD-1 therapy in metastatic melanoma. *Cell* 2016;165:35–44.
- 35 Rautela J, Dagley LF, de Oliveira CC, *et al.* Therapeutic blockade of activin-A improves NK cell function and antitumor immunity. *Sci Signal* 2019;12:eaat7527.
- 36 Shanker A, Verdeil G, Buferne M, *et al.* CD8 T cell help for innate antitumor immunity. *J Immunol* 2007;179:6651–62.
- 37 Uzhachenko RV, Shanker A. CD8⁺ T lymphocyte and NK cell network: circuitry in the cytotoxic domain of immunity. *Front Immunol* 2019;10:1906.
- 38 Petraglia F, Sacerdote P, Cossarizza A, *et al.* Inhibin and activin modulate human monocyte chemotaxis and human lymphocyte interferon-gamma production. *J Clin Endocrinol Metab* 1991;72:496–502.
- 39 Semitekolou M, Alissafi T, Aggelakopoulou M, *et al.* Activin-A induces regulatory T cells that suppress T helper cell immune responses and protect from allergic airway disease. *J Exp Med* 2009;206:1769–85.
- 40 Huber S, Stahl FR, Schrader J, *et al.* Activin A promotes the TGF-beta-induced conversion of CD4+CD25- T cells into Foxp3+ induced regulatory T cells. *J Immunol* 2009;182:4633–40.
- 41 Shurin MR, Ma Y, Keskinov AA, *et al.* BAFF and April from activin A-treated dendritic cells upregulate the antitumor efficacy of dendritic cells in vivo. *Cancer Res* 2016;76:4959–69.
- 42 Semitekolou M, Morianos I, Banos A. Dendritic cells conditioned by activin A-induced regulatory T cells exhibit enhanced tolerogenic properties and protect against experimental asthma. *J Allergy Clin Immunol* 2018;671–84.
- 43 Sierra-Filardi E, Nieto C, Domínguez-Soto A, *et al.* Ccl2 shapes macrophage polarization by GM-CSF and M-CSF: identification of CCL2/CCR2-dependent gene expression profile. *J Immunol* 2014;192:3858–67.
- 44 Tu MM, Abdel-Hafiz HA, Jones RT, *et al.* Inhibition of the CCL2 receptor, CCR2, enhances tumor response to immune checkpoint therapy. *Commun Biol* 2020;3:1–12.
- 45 House IG, Savas P, Lai J, *et al.* Macrophage-derived CXCL9 and CXCL10 are required for antitumor immune responses following immune checkpoint blockade. *Clin Cancer Res* 2020;26:487–504.
- 46 Mikucki ME, Fisher DT, Matsuzaki J, *et al.* Non-redundant requirement for CXCR3 signalling during tumoricidal T-cell trafficking across tumour vascular checkpoints. *Nat Commun* 2015;6:1–14.
- 47 Kuo PT, Zeng Z, Salim N, *et al.* The role of CXCR3 and its chemokine ligands in skin disease and cancer. *Front Med* 2018;5:271.
- 48 Harlin H, Meng Y, Peterson AC, *et al.* Chemokine expression in melanoma metastases associated with CD8⁺ T-cell recruitment. *Cancer Res* 2009;69:3077–85.
- 49 Mullins IM, Slingluff CL, Lee JK, *et al.* CXC chemokine receptor 3 expression by activated CD8⁺ T cells is associated with survival in melanoma patients with stage III disease. *Cancer Res* 2004;64:7697–701.
- 50 Tripathi C, Tewari BN, Kanchan RK, *et al.* Macrophages are recruited to hypoxic tumor areas and acquire a pro-angiogenic M2-polarized phenotype via hypoxic cancer cell derived cytokines oncostatin M and eotaxin. *Oncotarget* 2014;5:5350–68.
- 51 Korbecki J, Kojder K, Simińska D, *et al.* CC chemokines in a tumor: a review of pro-cancer and anti-cancer properties of the ligands of receptors CCR1, CCR2, CCR3, and CCR4. *Int J Mol Sci* 2020;21:8412.

SUPPLEMENTARY MATERIALS

Activin-A impairs CD8 T cell-mediated immunity and immune checkpoint therapy response in melanoma

Katarina Pinjusic^{1*}, Olivier A. Dubey^{1*}, Olga Egorova¹, Sina Nassiri^{1,2}, Etienne Meylan^{1,3,4,5}, Julien Faget^{1,6}, and Daniel B. Constam¹.

¹ Ecole Polytechnique Fédérale de Lausanne (EPFL) SV ISREC, Station 19, CH-1015 Lausanne, Switzerland

² Bioinformatics Core Facility, SIB Swiss Institute of Bioinformatics, CH-1015 Lausanne, Switzerland

³ Laboratory of Immuno-Oncology, Bordet Cancer Research Laboratories, Institut Jules Bordet, Faculty of Medicine, Université Libre de Bruxelles, 1070 Anderlecht, Belgium

⁴ Laboratory of Immunobiology, Faculty of Sciences, Université Libre de Bruxelles, 6041 Gosselies, Belgium

⁵ ULB Cancer Research Center (U-CRC) and ULB Center for Research in Immunology (U-CRI)

⁶ Present address: IRCM, Inserm, Univ Montpellier, ICM, Montpellier, France, INSERM U1194, Montpellier, France

* These authors contributed equally to this work

Corresponding author: Daniel B Constam, +41 21 693 07 41, Daniel.Constam@epfl.ch

SUPPLEMENTARY MATERIALS AND METHODS

SUPPLEMENTARY REFERENCES

SUPPLEMENTARY TABLES

Supplementary Table 1. Activin-A induced changes in the B16-F1 TME

Supplementary Table 2. qPCR primers

Supplementary Table 3. Antibodies used for immune-profiling

SUPPLEMENTARY FIGURES

Supplementary Figure 1. Effects of *INHBA* on the composition, cell proliferation, and gene expression of immune infiltrates in B16-F1 melanoma.

Supplementary Figure 2. Antigen cross-presentation in blood and lymphoid organs and analysis of CD4/CD8 cell depletion in B16.OVA- β A melanoma-bearing mice.

Supplementary Figure 3. Analysis of *in vitro* activated T cells and their effect on tumor immune infiltrates after adoptive transfer in B16-F1 melanoma-bearing mice.

Supplementary Figure 4. Characterization of YUMM3.3 and iBIP2 2891L cell lines.

Supplementary Figure 5. Activin-A accelerates melanoma growth independently of CSF1R⁺ TAMs.

Supplementary Figure 6. Activin-A directly impairs CXCL9/10 production by immortalized cDC1 cells.

Supplementary Figure 7. Expression of immune regulators that were not modulated by melanoma-derived Activin-A.

Supplementary Figure 8. Correlation of *INHBA* expression with the survival of melanoma patients.

Supplementary Figure 9. Gating strategy for TIL profiling by a 16-color flow cytometry antibody panel.

Supplementary Figure 10. Gating strategy used to analyze OVA-specific T cells and SIINFEKL presentation by APCs in figures 2 and S2.

Supplementary Figure 11. Gating strategy used for ATCT analyses in Fig. 3 and S3.

Supplementary Figure 12. Gating strategy used in Fig. 5 and S7 to analyze CXCL9 expression in tumors.

SUPPLEMENTARY MATERIALS AND METHODS

Cell lines

For all cell lines, culture media were supplemented with 10% fetal bovine serum, 50 µg/mL gentamicin (Gibco, Thermo Fisher Scientific, Waltham, MA, USA), and 1% GlutaMAX (Gibco). B16F1, HepG2, and HEK293T cells were purchased from ATCC and maintained in DMEM (Sigma-Aldrich, St. Louis, MO, USA). YUMM3.3 cells were provided by Dr. Anna Obenauf (Vienna, AU) and maintained in DMEM/F12 (Gibco). iBIP2 cell lines were provided by Mélanie Tichet (Hanahan lab, EPFL, Lausanne, CH) and maintained in RPMI in presence of 1 µg/mL doxycycline (Sigma-Aldrich). B16-F0 cells expressing lentiviral ovalbumin (B16.OVA) have been described [1]. HepG2 reporter cells were established by stable lentiviral transduction of a CAGA-Luc reporter and Renilla luciferase for normalization [2]. All cell lines were regularly tested negative for Mycoplasma (SouthernBiotech, Birmingham, AL, USA, 13100-01 or Biontex, Munich, DE, M020), and authenticated by the presence or absence of pigmentation, cell shapes, and unique responses of characteristic luciferase reporters or Dox-inducible transgenes.

Expression vectors and cloning

A Spe1 fragment of INHBA cDNA (NM_002192.2, nucleotides 218-1609, plus myc tag) was subcloned into XbaI-digested pLenti-EF1alpha-MCS-SV40-puro vector [3]. pLenti-EF1alpha-ActA-SV40-bsd was generated by subcloning INHBA from pLenti EF1a-MycActA SV40puro into pLenti EF1a-OVA bsd. In brief, the INHBA coding sequence was PCR-amplified using the primers 5'-GGGGAGATCTAAGGCAATCACAACTTTTGC-3' and 5'-CACAGGGTCGACCACTGGTC-3' that introduced a Bgl II site at the 5' end. The resulting fragment was digested with BglII/MluI and inserted into BglII/MluI-digested pLenti EF1a-OVA bsd. pLenti-EF1alpha-AIIB-Fc-SV40-bsd and pLenti-EF1alpha-Mock-Fc-SV40-bsd were cloned using the same strategy, but using the primers 5'-GGGGAGATCTGCCTCGAGAATTGCTTCCAC-3' and 5'-GGGTCGACCACTGGT CGAC-3'.

Lentiviral transduction

YUMM3.3-Ctrl and - β A, iBIP2-Mock-Fc and -AIIB-Fc, B16F1-Ctrl.OVA and - β A.OVA cell lines were generated as previously described for B16F1-Ctrl and - β A [3]. In short, HEK293T cells were co-transfected with CMV Δ R8.74 (Addgene, Watertown, MA, USA 22036), pMD2.VSVg (Addgene 12259) mycINH β A, AIIB-Fc, OVA or empty transfer plasmid. Lentiviral particles were collected from filtered culture supernatant by ultracentrifugation and resuspended in sterile PBS. Target cells were transduced in a 12-well plate. YUMM3.3, iBIP2, and B16F1 cells were selected using blasticidin.

Reporter assay

HepG2 CAGA-Luc reporter cells [2] were seeded in 96-well plate and treated with 20 ng/mL recombinant Activin-A (R&D Systems, Minneapolis, MN, USA) as a positive control or with supernatant from INHBA- or Ctrl-transduced melanoma cells. Where indicated, 250 ng/mL of Follistatin (R&D Systems) was added to the cell condition medium. After overnight incubation, cell proteins were extracted in potassium phosphate buffer containing 0.5% Triton X-100. Luminescence of Firefly and Renilla luciferase was measured in 5 μ L of the extract by Centro LB960 luminometer in a white 96-well plate (Nunc 96 MicroWell™ Plates #236108) by the addition of 50 μ L P/R A (Firefly) and P/R B (Renilla) reagents [4]. Relative light units (RLU) represent firefly expression normalized to renilla and expressed relative to the non-treated control.

Cell viability assay

Cells were plated in 96-well plates at a density of 5×10^3 cells/well and cultured for 3 days. Alamar blue reagent (Invitrogen, DAL1025) was added to 90% confluent cells and fluorescence was measured 4 hrs later on a TECAN spectrophotometer at the emission wavelength of 590 nm after excitation at 560 nm.

Western blot analysis

Cells were lysed in a homemade RIPA buffer supplemented with the protease inhibitor cocktail (Roche, Basel, CH) and phosphatase inhibitors (Sigma-Aldrich). The conditioned medium was precipitated using ice-cold acetone and resuspended in RIPA buffer. Protein concentration was

measured by BCA assay (Thermo Fisher Scientific). Proteins were separated on 9-12% SDS-PAGE gels under reducing or non-reducing conditions and transferred on nitrocellulose membranes. Membranes were blocked with 5% skim milk (Sigma) in Tris-buffered saline containing 0.1% Tween-20, before incubation with primary antibodies against phosphorylated or total SMAD2 (Cell Signaling 8828, and 3103), γ -tubulin (Sigma GTU88), GAPDH (Abcam ab70699, Cambridge, UK), Activin-A (Abcam ab89307), Ovalbumin (Milipore AB1225, Burlington, MA, USA) for 2 hrs at room temperature or overnight at 4°C. For fluorescence detection, proteins were visualized on an Odyssey CLx instrument after incubation with a secondary antibody coupled with IRDye 800CW and IRDye 680RD (all from Licor, Lincoln, NE, USA). Chemiluminescence was revealed on X-ray film (Kodak, Rochester, NY, USA) or ChemiDoc MP (Biorad, Hercules, CA, USA) using HRP-coupled secondary antibodies and ECL reagents (Thermo Fisher).

Quantitative polymerase chain reaction

Cells were cultured in 6-well plates and RNA was extracted using the ReliaPrep RNA Cell Miniprep System (Promega, Madison, WI, USA) following the manufacturer's protocol. For total tumor RNA extraction, snap-frozen tumor pieces were sonicated or homogenized in 1 mL of QIAzol (Qiagen, Hilden, DE), and followed by chloroform extraction. Total RNA was isolated using the RNeasy mini kit (Qiagen) according to the manufacturer's protocol. cDNA was synthesized from 1 μ g RNA using the PrimeScript RT-PCR Kit (Takara, Kusatsu, JP). The analysis was performed using the SYBR Green GoTaq Master Mix (Promega) on a QuantStudio 6 instrument (Applied Biosystems, Waltham, MA, USA). qPCR primers are listed in **Table S2**.

Melanoma grafts and adoptive T cell transfers

B16F1, B16.OVA, B16F1.OVA, YUMM3.3: 10^5 cells were injected intradermally (B16F1 & B16.OVA) or 2.5×10^5 cells subcutaneously (YUMM3.3), or 8×10^5 cells subcutaneously (B16F1-OVA) into the right flank of 8-12 week old female C57BL/6 mice (Charles River laboratories) [1]. Alternatively, 8-12 week old male FVB/N mice (Charles River, Wilmington, MA, USA) received 10^5 iBIP2 2891L cells subcutaneously the day after they were switched to 0.625 g/Kg Doxycycline Hyclat food pellets (Safe, E8404 Version 0002_150) to activate the rtTA-induced

expression of BRAF V600E [5]. Rag1^{-/-} mice were bred at EPFL. For OT-I adoptive T cell transfer, OT-I CD45.1 splenocytes were activated 5 days in vitro as described below. Before the transfer, T cells were extensively washed in PBS and dead cells were removed using the dead cell removal kit (Miltenyi Biotec, 130-090-101, Bergisch Gladbach, DE) following the manufacturers instruction. 1×10^6 activated OT-I T cells in 100 μ l PBS, or PBS alone were injected i.v. per mice on day 7 after the tumor challenge. Tumors were measured 3 times/week and volumes were calculated using the formula $V = [1.58\pi \times (\text{length} \times \text{width})^3]/6$ [6].

Quantification of Activin-A plasma levels

At the experimental endpoint, blood was collected in heparin-coated tubes (Microvette 500 LH, SARSTEDT AG & Co.). Plasma was separated by centrifugation and aliquoted into new Eppendorf tubes. Activin-A levels in plasma were quantified by ELISA following the manufacturer's instructions (R&D DAC00B).

Antibody injections

To deplete T cells, mice were intraperitoneally injected with 10 mg/kg anti-CD4 (clone YTS191) and/or anti-CD8 (clone YTS169.4), or rat IgG2b (clone LTF-2, all from BioXcell, Lebanon, NH, United States) in 200 μ L PBS twice weekly, starting one day before tumor grafting. For anti-CSF1R depletion, treatment of YUMM3.3 was initiated one day before the tumor graft and administered twice weekly thereafter. Mice were treated with 50 mg/kg i.p. rat anti-CSF1R (clone AFS98, BioXCell) or control rat IgG2a antibody (clone 2A3, BioXCell). For anti-PD1 and anti-CTLA4 pre-clinical studies, mice were intraperitoneally injected every 3 days with 10 mg/kg anti-PD1 (clone RMP1-14), 5 mg/kg anti-CTLA4 (clone 9H10), or 10 mg/kg rat IgG2a and 5 mg/kg Syrian hamster IgG (all from BioXcell) in 200 μ L PBS. For anti-IL4 injections, mice were treated with 1mg of anti-IL4 (clone 11B11, BioXcell) or rat IgG (clone HRPN, BioXcell) one day before the tumor injections, followed by 500 μ g every 5 days. All procedures were according to Swiss legislation and approved by the cantonal veterinary administration.

Tumor dissociation and flow cytometry analyses

Tumors were dissected, minced using rounded scissors, and digested in Dnase I (0.02 mg/mL, Sigma) and collagenase (1 mg/mL, Sigma) in RPMI using a gentleMACS Octo Dissociator

(Miltenyi). Red blood cells were lysed using PharmLyse buffer (BD Biosciences). Cells were washed with PBS and $1-5 \times 10^6$ of cells were used for staining. Cells were incubated with mouse FcR blocking solution (1:200, Miltenyi) and Live/Dead fixable blue dead cell stain (1:1000, Life Technologies, Carlsbad, CA, USA) for 30 min. After washing, cells were stained for surface markers for 45 min in FACS buffer (2% FBS, 2 mM EDTA in PBS). For dextramer staining, 2 μ L MHC-I SIINFEKL dextramers (Immudex, Copenhagen, DK) were added before antibody staining. MHC-I SIYRYYGL dextramer was used as a negative control. For intracellular cytokine staining, 10^6 cells were plated in the complete RPMI medium and incubated for 5 hrs with eBioscience™ Cell Stimulation Cocktail (00-4970-93) and protein transport inhibitor (BD 555029). Cells were then washed and stained for surface markers, followed by fixation and permeabilization using the FoxP3 staining buffer set (eBioscience) before intracellular staining. After the staining, cells were collected in FACS buffer, and data were acquired using an LSRII SORP or an LSR Fortessa cytometer (Becton Dickinson, Franklin Lakes, NJ, USA). Antibodies used for 16-color panel and other stainings are listed below in **Table S3** [7].

To quantify OT-I cells, tumors were weighed, digested, and resuspended in 100 μ l PBS per 50 mg of a tumor. Single-cell suspensions of draining lymph nodes were obtained by pressing the lymph node against the mesh of a cell strainer. Dissociated cells were washed and resuspended in 500 μ l PBS. 100 μ l of tumor and 200 μ l of lymph node cell suspension were used for antibody staining. Stained samples were resuspended in 200 μ l FACS buffer and loaded on Precision Count Beads (25 μ l, BioLegend 424902, San Diego, CA, USA). Data were acquired on an LSR Fortessa cytometer using beads as a stopping gate. OT-I cell numbers were calculated following the manufacturer's instructions. For intracellular CXCL9 staining, tumors were dissociated and single-cell suspensions were incubated for 3h with protein transport inhibitor (BD 555029) without additional stimulation and stained for intracellular CXCL9 as described above for intracellular cytokines. Gating strategies are provided in **Supplementary Figures 9-12**.

In vitro T cell activation and cytotoxicity assay

Splenocytes were collected from OT-I CD45.1 transgenic mice. Red blood cells were lysed using RBC lysis buffer, and 5×10^6 cells/mL activated with 10 μ g/mL of SIINFEKL peptide (Sigma

Aldrich S7951) and 10 ng/mL rhIL-2 (Peprotech 200-02, East Windsor, NJ, United States) for 3-5 days in the T-cell medium. Where indicated, cells were activated in presence of 20-100 ng/mL recombinant Activin-A (R&D Systems) or treated with 20 ng/ml TGFβ1 (Gibco). The T-cell medium was prepared by supplementing the RPMI with 10% heat-inactivated FBS, 1% PS, 1 mM sodium pyruvate, 50 μM Beta-ME, 100 μM non-essential amino acids, 10 mM HEPES followed by sterile filtration. To analyze activation markers, OT-I T cells from individual spleens were expanded independently from each other for each experiment and stained with different panels of antibodies, resulting in some variability in baseline fluorescence intensities. Therefore, the signals after Activin-A treatment were normalized to each individual corresponding control. Source data without normalization are shown as Supplementary information. For killing assays, activated T cells were washed and rested for 6 hrs in a medium without cytokines. 1×10^6 tumor cells/mL PBS were stained with 1 μL/mL Cell Trace CFSE (ThermoFisher C34554) for 20 min at 37°C and washed before overnight co-culture with activated OT-I T cells at the indicated ratios. To quantify the killing of tumor cells by OT-I T cells, co-culture supernatant and adherent cells were collected. Samples were stained using Annexin V-APC Apoptosis Detection Kit with PI (Biolegend 640932) following the manufacturer's protocol and fluorescence signals were acquired using LSRII SORP or an LSR Fortessa cytometer (Becton Dickinson). Tumor cell killing percentage is calculated as = (% of live tumor cells - % of live cells in tumor only control) / % of live cells in tumor only control x 100.

Cytokine and chemokine quantification

Tumors were dissected, minced using rounded scissors, and digested in DNase-I (0.02 mg/mL, Sigma) and collagenase (1 mg/mL, Sigma) in RPMI using a gentleMACS Octo Dissociator (Miltenyi). After washing and counting with a TC20 automated cell counter (Bio-Rad) 5×10^6 cells/mL were cultured in 96-well plates for 28 hrs in the complete DMEM-F12 medium. Factors secreted into the culture supernatant were cleared from cells and debris by centrifugation and stored at -80°C until analyses. The supernatants were analyzed undiluted or diluted 70x and 13 secreted cytokines and chemokines were analyzed using LEGENDplex™ Mouse Th Cytokine Panel (13-plex) and LEGENDplex™ Mouse Proinflammatory Chemokine Panel (13-plex) (both from BioLegend) following manufacturer's protocol, respectively. Data were

acquired using an LSR Fortessa cytometer (Becton Dickinson) and analyzed using BioLegend's LEGENDplex™ Data Analysis Software (BioLegend).

Mouse cDC1 cell line culture and activation

Immortalized mouse cDC1 cells [8] were cultured in IMDM medium supplemented with 10% heat-inactivated FBS, 100x Glutamax, 10 mM HEPES, 100 μ M Pen/Strep, 50 μ M β -mercaptoethanol at 37° and 5% CO₂. PBS supplemented with 20 mM HEPES and 5 mM EDTA was used for cell passaging. For activation, 250'000 cells were seeded per well in a 12 well plate and incubated for 24 hrs with 5 μ g/ml LPS and 10 ng/ml IFN γ . Where indicated, cells were also incubated with 50 ng/ml recombinant Activin-A, TGF β , or BMP4 (all from R&D), or 10 μ M SB431542 (Tocris Bioscience). During the last 3 hrs of incubation, Golgi Plug (BD 555029) was added to the cells followed by intracellular cytokine staining using the protocol described above. Supernatants were collected for CXCL9 and CXCL10 quantification by ELISA following the manufacturer's instructions (Abcam ab203364 and ab260067, respectively).

Bioinformatics analysis

The association between the expression levels of INHBA mRNA and response to anti-PD1 therapy was assessed using a previously published RNA-seq dataset [9]. Processed data and metadata were obtained from Gene Expression Omnibus (GEO) and visualized in R. One-way ANOVA was not significant when comparing complete response, partial response, and progressive disease samples. By pooling the complete and partial responses into one group, we found a significant difference between responders and non-responders using Welch two sample t-test. Kaplan-Meier survival curves comparing TCGA melanoma patients stratified by the expression level of the INHBA gene were obtained from TIMER database (<http://timer.cistrome.org/>). To assess the correlation between INHBA expression levels and melanoma disease stage or driver mutations, processed data was obtained from UCSC's Xena browser (<https://tcga.xenahubs.net/>), and visualized in R. Expression of INHBA in different cell types within the TME was examined using a publicly available single-cell RNA-seq data [10] (GSE72056). Processed data including the original cell type annotations was obtained from GEO and visualized in R.

Statistical analysis

Statistical tests were performed using the Prism software (GraphPad). Unless indicated, data represent the mean \pm SEM of at least 2 independent experiments. When comparing two groups, normal distributions were analyzed by the Shapiro-Wilk normality test, and p-values calculated by Student's t-test (normal distribution) or Mann-Whitney's test (non-parametric test). One-way ANOVA was used to compare several groups of unpaired values. Kaplan-Meier survival curves were analyzed using the Gehan-Breslow-Wilcoxon test. Data points identified as outliers by the regression and outlier (ROUT) removal method in Prism 9 with a False Discovery Rate \leq 1% were excluded. Power Analysis was waved by the animal experimentation authorities due to pre-existing data about the effect sizes of Activin-A induced tumor growth and cachexia. Tumor volumes at the endpoint were compared by ANOVA or Student's t-test, as indicated in the figure legends.

SUPPLEMENTARY REFERENCES

1. Faló LD, Kovacsovics-Bankowski M, Thompson K, Rock KL. Targeting antigen into the phagocytic pathway in vivo induces protective tumour immunity. *Nat Med* [Internet]. Nature Publishing Group; 1995 [cited 2021 Jun 4];1:649–53. Available from: <http://www.nature.com/naturemedicine>
2. Fuerer C, Nostro MC, Constam DB. Nodal^{1/2} Gdf1 Heterodimers with Bound Prodomains Enable Serum-independent Nodal Signaling and Endoderm Differentiation. *J Biol Chem* [Internet]. in Press; 2014 [cited 2017 Jul 19];289:17854–71. Available from: <https://www.ncbi.nlm.nih.gov/pmc/articles/PMC4067217/pdf/zbc17854.pdf>
3. Donovan P, Dubey OA, Kallioinen S, Rogers KW, Muehlethaler K, Müller P, et al. Paracrine Activin-A signaling promotes melanoma growth and metastasis through immune evasion. *J Invest Dermatol* [Internet]. 2017;137:2578–87. Available from: <https://www.ncbi.nlm.nih.gov/pubmed/28844941>
4. Hampf M, Gossen M. A protocol for combined Photinus and Renilla luciferase quantification compatible with protein assays. *Anal Biochem* [Internet]. Academic Press Inc.; 2006 [cited 2020 Nov 9];356:94–9. Available from: <https://pubmed.ncbi.nlm.nih.gov/16750160/>
5. Neubert NJ, Schmittnaegel M, Bordry N, Nassiri S, Wald N, Martignier C, et al. T cell-induced CSF1 promotes melanoma resistance to PD1 blockade. *Sci Transl Med* [Internet]. 2018;10:eaan3311. Available from: <http://stm.sciencemag.org/content/10/436/eaan3311.short>
6. Feldman JP, Goldwasser R. A Mathematical Model for Tumor Volume Evaluation Using Two-Dimensions. *Jpurnal Appl Quant methods*. 2009;4:455–62.
7. Faget J, Groeneveld S, Boivin G, Sankar M, Zangger N, Garcia M, et al. Neutrophils and Snail Orchestrate the Establishment of a Pro-tumor Microenvironment in Lung Cancer. *Cell Rep* [Internet]. Elsevier B.V.; 2017 [cited 2021 Jun 14];21:3190–204. Available from: <https://pubmed.ncbi.nlm.nih.gov/29241546/>
8. Fuertes Marraco SA, Grosjean F, Duval A, Rosa M, Lavanchy C, Ashok D, et al. Novel murine dendritic cell lines: A powerful auxiliary tool for dendritic cell research. *Front Immunol*.

Frontiers; 2012;3:331.

9. Hugo W, Zaretsky JM, Sun L, Song C, Moreno BH, Hu-Lieskovan S, et al. Genomic and Transcriptomic Features of Response to Anti-PD-1 Therapy in Metastatic Melanoma. *Cell* [Internet]. Elsevier Inc.; 2016;165:35–44. Available from:

<http://dx.doi.org/10.1016/j.cell.2016.02.065>

10. Tirosh I, Izar B, Prakadan SM, Wadsworth MH, Treacy D, Trombetta JJ, et al. Dissecting the multicellular ecosystem of metastatic melanoma by single-cell RNA-seq. *Science* (80-). 2016;352:189–96.

SUPPLEMENTARY TABLES

Supplementary Table 1. Activin-A induced changes in the B16-F1 TME

Population	Markers	Ctrl	β A	p-value
CD45+ leukocytes	CD45+	26.9% \pm 7.6%	15.1% \pm 8.7%	0.065
CD11b+ myeloid cells	CD11b+	51.4% \pm 17.8%	70.8% \pm 3.8%	0.0004
mMDSCs	CD11b+Ly6Chi	13.8% \pm 6.5%	23.8% \pm 6.7%	0.004
Macrophages	CD11b+F4/80+	12.7% \pm 4.1%	17.3% \pm 8.4%	0.17
Macrophage CD206 MFI	CD206	17142 \pm 7961	25501 \pm 5789	0.068
Neutrophils	CD11b+Ly6G+	4.5% \pm 6.7%	4.3% \pm 2.5%	0.24
Dendritic cells	CD11c+F4/80-	13.0% \pm 6.3%	21.4% \pm 4.4%	0.003
Dendritic cells MHC-II MFI	IA/IE	31396 \pm 8305	30757 \pm 4751	0.84
Dendritic cells CD80	CD80	1216 \pm 3853	3853 \pm 758	<0.0001
NK cells	NK1.1+CD3-	15.8% \pm 12.1%	5.1% \pm 2.9%	0.006
CD8 T-cells	CD3+CD8+	7.1% \pm 4.0%	2.4% \pm 1.0%	0.001
Tconv	CD3+CD4+FoxP3-	2.9% \pm 1.4%	5.0% \pm 2.2%	0.04
Tregs	CD3+CD4+FoxP3+	1.7% \pm 0.8%	1.6% \pm 1.6%	0.41
B-cells	CD19+B220+	1.1% \pm 0.8%	3.4% \pm 3.0%	0.07

Supplementary Table 2. qPCR primers

Primer Name	Sequence	Species
Gapdh fw	ACTGAGGACCAGGTTGTCTCC	Mus musculus
Gapdh rv	GTTGGGATAGGGCCTCTCTTGC	Mus musculus
Acvr1b fw	GGGTGGGGACCAAACGATAC	Mus musculus
Acvr1b rv	TCGGAGGGCACTAAGTCGTA	Mus musculus
Acvr1c fw	AGACGGTGATGCTGAGACACGA	Mus musculus
Acvr1c rv	GACCATTCCAGCCACAGTCACT	Mus musculus
Acvr2b fw	ATTGCTACGACAGGCAGGAG	Mus musculus
Acvr2b rv	GTGGCTCGTACGTGACTTCT	Mus musculus
Acvr2a fw	AAGTTCGAGGCTGGCAAGTCTG	Mus musculus
Acvr2a rv	CCTCAGAAATGCGTCCCTTTGG	Mus musculus
IFNy fw	TGAACGCTACACACTGCATCTTGG	Mus musculus
IFNy rv	CGACTCCTTTTCCGCTTCCTGAG	Mus musculus
IL10 fw	GCTCTTACTGACTGGCATGAG	Mus musculus
IL10 rv	CGCAGCTCTAGGAGCATGTG	Mus musculus
IL1b fw	TGCCACCTTTTGACAGTGATGAGA	Mus musculus
IL1b rv	TCATCAGGACAGCCCAGGTCA	Mus musculus
IL6 fw	ACCACGGCCTTCCCTACTTC	Mus musculus
IL6 rv	TTGCCATTGCACAACCTCTTTTCTCA	Mus musculus
TNFa fw	CCCACGTCGTAGCAAACCA	Mus musculus
TNFa rv	ACAAGGTACAACCCATCGGC	Mus musculus
IL2 fw	ACTAAAGGGCTCTGACAACAC	Mus musculus
IL2 rv	CCTCAGAAAGTCCACCACAGT	Mus musculus
Perforin fw	ACACAGTAGAGTGTGCGATGTAC	Mus musculus
Perforin rv	GTGGAGCTGTTAAAGTTGCGGG	Mus musculus
Granzyme B fw	CAGGAGAAGACCCAGCAAGTCA	Mus musculus
Granzyme B rv	CTCACAGCTCTAGTCCTCTTGG	Mus musculus
Inhba fw	CCTCTGGCTATCACGCCAAT	Mus musculus
Inhba rv	ACATGGGTCTCAGCTTGGTG	Mus musculus
Fst fw	AGTAAGTCGGATGAGCCGGT	Mus musculus
Fst rv	TTCACTTCAAGAAGCACGCC	Mus musculus

Supplementary Table 3. Antibodies used for immune-profiling

Reagent	Source	Clone	Reference
CD103 PE	eBioscience	2.00E+07	12-1031-82
CD11b BV711	BioLegend	M1/70	101241
CD11c BV421	BioLegend	N418	117330
CD172a (SIRPα) PerCP/Cy5.5	eBioscience	P84	144009
CD19 BV510	BioLegend	6D5	115545
CD197 (CCR7) AlexaFluor488	eBioscience	4B12	120112
CD206 FITC	BioLegend	C068C2	141703
CD25 APCeFluor780	eBioscience	PC61.5	47-0251-82
CD25 PE	BioLegend	PC61	102007
CD3 APC-eFluor780	eBioscience	500A2	47-0033-82
CD3 PE	BioLegend	145-2C11	100308
CD3e PE-Cy5.5	eBioscience	145-2C11	35-0031-82
CD4 BV785	BioLegend	RM4-5	100552
CD4 PE-Cy7	eBioscience	GK1.5	25-0041-82
CD45 APC	eBioscience	30-F11	17-0451-82
CD45 PerCP	BioLegend	30-F11	103129
CD45.1 BV421	BioLegend	A20	110731
CD45.2 BUUV737	BD Horizon	104	564880
CD45R (B220) APC	Miltenyi	RA3-6B2	130-102-259
CD69 BV711	BioLegend	H1.2F3	104537
CD8 BV510	BD Horizon	53-6.7	563068
CD80	Miltenyi	16-10A1	130-102-372
CXCL9 (MIG) AlexaFluor647	eBioscience	MIG-2F5.5	515606
F4/80 BV605	BioLegend	BM8	123133
FoxP3 PE-eFluor610	eBioscience	FJK-16s	61-5773-82
GranzymeB AlexaFluor647	BioLegend	GB11	515406
H2Kb FITC	BioLegend	AF6-88.5	116505
H2Kb-SIINFEKL APC	BioLegend	25-D1.16	141605
IA/IE (MHC-II) AlexaFluor700	BioLegend	M5/114.15.2	107622
IA/IE (MHC-II) APC-Cy7	BioLegend	M5/114.15.2	107627
IFNγ PE	BioLegend	XMG1.2	505808
Ki67 eFluor450	Invitrogen	SoIA15	48-5698-80
Ly6C AlexaFluor700	BioLegend	HK1.4	128023
Ly6C PerCP/Cy5.5	BioLegend	HK1.4	128012
Ly6G FITC	BioLegend	1A8	127605
Ly6G PE	BioLegend	1A8	127607
NK1.1 BV650	BioLegend	PK136	108735
PD1 PE/Cy7	BioLegend	RMP1-30	109109
TNFα PE-Cy7	BioLegend	MP6-XT22	506323
XCR1 APC/Cy7	eBioscience	ZET	148223

SUPPLEMENTARY FIGURES

Supplementary Figure 1. Effects of *INHBA* on the composition, cell proliferation, and gene expression of immune infiltrates in B16-F1 melanoma.

A, Circulating Activin-A plasma concentrations in B16F1-Ctrl or - β A tumor-bearing mice quantified by ELISA. Error bars, SEM (n = 5 per group); **p<0.01, Student's t-test. **B-H**, qPCR analyses of (B) *Gzmb*, (C) *Perf1*, (D) *Il1b*, (E) *Il2*, (F) *Il10*, (G) *Ifng*, and (H) *Tnfa*, in whole tumor extracts normalized to *Gapdh* expression (n = 6-7 Ctrl, and 10 β A tumors). **I**, Percentage of B cells (B220⁺CD19⁺) in CD45⁺ cells in tumors (n = 4 Ctrl, 7 β A tumors). **J-M**, Quantification of Ki67⁺ proliferating cells in dissociated B16F1-Ctrl or - β A tumors stained by flow cytometry for (J) CD3⁺CD8⁺, (K) CD3⁻NK1.1⁺, (L) CD4⁺FoxP3⁺, (M) CD4⁺FoxP3⁻, Error bars, SEM (n = 7-9); *p<0.05, **p<0.01, ***p<0.001, ****p<0.0001, Student's t-test. **N**, Summary of *INHBA*-induced changes observed in the TME of B16-F1 melanoma.

Supplementary Figure 2. Antigen cross-presentation in blood and lymphoid organs and analysis of CD4/CD8 cell depletion in B16.OVA- β A melanoma-bearing mice.

A, H2Kb expression (left) and H2Kb-SIINFEKL presentation (right) in B16.OVA-Ctrl and - β A stable cell lines treated with or without 20 μ g/mL IFN γ for 24 hrs. Western blot of OVA and γ -tubulin expression in B16.OVA-Ctrl and - β A stable cell lines. **B**, As in (A), but for B16F1-Ctrl.OVA and - β A.OVA cell lines. **C-F**, Flow cytometric analysis of the frequency of (C) CD11c⁺ and (D) CD11c⁺CD8⁺ APCs in CD45⁺, and (E) H2Kb-SIINFEKL presentation by CD11c⁺ APCs, and (F) H2Kb expression in CD11c⁺ APCs in dLNs of B16.OVA-Ctrl and B16.OVA- β A tumor-bearing mice (n = 4). **G-H**, Flow cytometry of (G) CD4⁺ and CD8⁺ T cells in blood and tumors of B16.OVA-Ctrl and - β A tumor-bearing mice, and (H) quantification of CD3⁺CD8⁺ T cells at the endpoint after injection of the indicated antibodies. Error bars, SEM (n = 4-5); *p<0.05, **p<0.01, ***p<0.001, ****p<0.0001, ordinary one-way ANOVA with Holm-Šídák correction for multiple comparisons.

Supplementary Figure 3. Analysis of *in vitro* activated T cells and their effect on tumor immune infiltrates after adoptive transfer in B16-F1 melanoma-bearing mice.

A, RT-qPCR analysis of *Acvr2a*, *Acvr2b*, *Alk4*, and *Alk7* mRNA expression in CD8-depleted splenocytes of naïve mice (-) and in *in vitro* differentiated CD8⁺ T cells (+), normalized to *Gapdh* mRNA expression. Error bars, SEM (n = 3 biological replicates); p-values, Student's t-test. **B**, Representative Western blots of pSmad2, total Smad2 and γ -tubulin (loading control) in naïve CD8⁺ T cells and CD8 negative splenocytes isolated from OT-I mice treated for 2 hrs with 20 ng/ml TGF β 1 or Activin-A (n = 3 experiments). **C**, Western blots of pSmad2, total Smad2, and *Gapdh* (loading control) in OT-I T cells stimulated during 4 days with 20 ng/ml Activin-A (ActA) or without (CTRL), together with OVA peptide (SIINFEKL) and IL2. Extracts of B16F1 cells treated without (-) or with doxycycline (Dox) to induce constitutively active mutant *Alk4* (caALK4) were used as controls [3]. **D**, Representative Western blots of pSmad2 and γ -tubulin (loading control) in OT-I T cells treated for 2h with 20 ng/ml TGF β or Activin-A after 4 days of *in vitro* activation (n = 3 independent experiments). **E**, Mean fluorescence intensities of CD25, CD69, and PD1 (n = 4 experiments) and TNF α , IFN γ , Granzyme B stainings in OT-I T cells (n = 3 experiments) that were activated during 4 days with or without Activin-A. Error bars, SEM; p-values, 2way ANOVA with Tukey's correction for multiple comparison. **F**, Comparison of B16.OVA and B16F1.OVA-Ctrl versus - β A tumor cell killing, and non-OVA B16 cell killing in 1:1 co-culture with activated OT-I T cells (n = 4-5 independent experiments). Error bars, SEM, p-values, ****p<0.0001, ordinary one-way ANOVA with Holm-Šídák correction for multiple comparisons **G-J**, Quantification of (G) CD45⁺, (H) CD11b⁺, (I) CD4⁺ T cells, and (J) endogenous CD45.2⁺CD8⁺ T cells per mg of B16F1-Ctrl.OVA or B16F1- β A.OVA tumor one week after the injection of activated OT-I T cells or PBS control. Error bars, SEM (n = 7-8), *p<0.05, **p<0.01, ***p<0.001, ****p<0.0001, ordinary one-way ANOVA with Holm-Šídák correction for multiple comparisons. **K-M**, Mean fluorescence intensity of (K) IFN γ , (L) Granzyme B, and (M) TNF α protein staining in OT-I T cells analyzed by flow cytometry one week after the transfer into B16F1-Ctrl.OVA or - β A.OVA tumor-bearing mice. Error bars, SEM (n=7-8); p<0.05, **p<0.01, ***p<0.001, ****p<0.0001 (Student's t-test).

Supplementary Figure 4. Characterization of YUMM3.3 and iBIP2 2891L cell lines.

A, RT-qPCR analyses of endogenous *Inhba* expression in B16F1 (n = 6), YUMM3.3 (n = 5), and iBIP2 2891L cells (n = 6) relative to *Gapdh* expression. **B**, Anti-Activin-A Western blot of B16F1, YUMM3.3, and iBIP2 2891L cell-conditioned media on non-reducing gels. Predicted molecular weights of myc-tagged Activin-A precursor (pro β A₂), hemicleaved form (pro β A: β A), and mature form (β A₂) are indicated. Asterisk marks endogenous mature Activin-A. UT: untransfected; Ctrl: Empty control lentivirus; β A: *myc-INHBA* lentivirus. **C**, RT-qPCR analyses of endogenous *Fst* expression in B16F1, YUMM3.3, and iBIP2 2891L cell lines relative to *Gapdh* expression (n = 3). **D**, CAGA-Luc induction in HepG2 reporter cells after overnight incubation with 0, 20, or 40 ng/ml Activin-A in the control medium or in the SN collected from YUMM3.3 cells (n = 2). **E**, CAGA-Luc induction after overnight incubation with iBIP2 2891L supernatant alone or in presence of an increasing concentration of YUMM3.3 supernatants. Error bars, SEM (n = 3). **F**, Alamar blue cell viability staining in YUMM3.3-Ctrl and - β A cell cultures, and in YUMM3.3 cells treated with 20 ng/ml Activin-A (top, n = 3-4), or in cultured iBIP2 2891L Mock-Fc and AIIB-Fc cells (below, n = 2); Error bars, SEM, *p<0.05, **p<0.01, ***p<0.001, ****p<0.0001, Student's t-test.

Supplementary Figure 5. Activin-A accelerates melanoma growth independently of CSF1R⁺ TAMs.

A-D, Frequency of (A) CD11b⁺, (B) CD11b⁺Ly6C^{hi}, (C) CD11b⁺F4/80^{hi}, and (D) CD11b⁺F4/80⁺ cells in CD45⁺ immune infiltrates from YUMM3.3-Ctrl versus -βA tumors (left), or from iBIP2 Mock-Fc versus A1IB-Fc tumors (right) analysed by flow cytometry at endpoints. **E**, Growth curves of YUMM3.3-Ctrl and -βA tumors treated with αCSF1R or control IgG antibodies. Error bars, SEM (n=4-5); *p<0.05, **p<0.01, ***p<0.001, ****p<0.0001, Student's t-test. **F**, The ratio of CD8/CD4 cells in the tumors shown in (E) at the endpoint. Error bars, SEM (n = 4-5); *p<0.05, **p<0.01, ***p<0.001, ****p<0.0001, 2-way ANOVA with Tukey's correction for multiple comparison. **G**, Representative flow cytometry gating panels (left), and quantification of F4/80^{hi} TAM depletion in YUMM3.3-Ctrl and -βA tumors (right) after αCSF1R or control IgG administration. **H-K**, Expression of (H) IFNγ and (I) TNFα in CD8⁺ T, and of (J) IFNγ and (K) TNFα in CD4⁺ T cells at the endpoint. Error bars, SEM (n = 4-5); *p<0.05, **p<0.01, ***p<0.001, ****p<0.0001, 2-way ANOVA with Tukey's correction for multiple comparison.

Supplementary Figure 6. Activin-A directly impairs CXCL9/10 production by immortalized cDC1 cells

A, Illustration of the experimental procedure. Immortalized mouse cDC1 cells [8] were activated with 5 μg/ml LPS + 10 ng/ml IFNγ and, where indicated, with 50 ng/ml ActA, TGFβ, BMP4, or 10 μM SB inhibitor during 24 hrs. Production of CXCL9 was analyzed by intracellular cytokine staining and flow cytometry after incubation with Golgi plug for 3 hrs. Secreted chemokines in the SN were quantified by ELISA. **B**, Histogram of one representative immunofluorescent staining (left panel), and quantification of the mean fluorescence intensity (MFI) of intracellular CXCL9 (right panel) in LPS-activated cDC1 cells that were treated as indicated (n = 3-5). **C, D**, Secretion of (C) CXCL9 and (D) CXCL10 in the SN of cDC1 cultures measured by ELISA (n = 3-4). **E**, Expression (MFI) of the cell proliferation marker Ki67 in cDC1 cells that were treated as indicated. Error bars, SEM (n = 2-4); *p<0.05, **p<0.01, ***p<0.001, ****p<0.0001, ordinary one-way ANOVA with Holm-Šidák correction for multiple comparisons. All MFI values were normalized to those of cells activated with LPS alone (control).

Supplementary Figure 7. Expression of immune regulators that were not modulated by melanoma-derived Activin-A.

A-P, Quantification of (A) CCL2, (B) CCL5, (C) CXCL5, (D) CCL3, (E) CCL4, (F) CCL20, (G) IL5, (H) IL2, (I) IL6, (J) TNF α , (K) IL9, (L) IL21, (M) IL13, (N) IL22, (O) IL17A, and (P) IL17F secreted from *ex vivo* cultured dissociated YUMM3.3-Ctrl (n = 5-6) and - β A tumors (n = 8). Error bars, SEM; *p < 0.05, **p < 0.01, ***p < 0.001, and ****p < 0.0001, Mann-Whitney test for non-parametric data and a two-tailed t-test for parametric data. **Q**, Relative *Tgfb1* mRNA levels in total YUMM3.3-Ctrl and - β A tumor extracts measured by RT-qPCR and normalized to *Gapdh*. Error bars, SEM (n = 4); p-value, Student's t-test. **R**, Growth curves of YUMM3.3-Ctrl and - β A tumors treated with α IL-4 or IgG and tumor volumes measured at the endpoint. Error bars, SEM (n = 4-5); *p < 0.05, **p < 0.01, ***p < 0.001, and ****p < 0.0001, ordinary one-way ANOVA with Holm-Šídák correction for multiple comparisons. **S**, Representative histograms showing CXCL9 expression in MoMac and DC subsets in YUMM3.3-Ctrl and - β A tumors.

Supplementary Figure 8. Correlation of *INHBA* expression with the survival of melanoma patients.

A, Survival of patients with *INHBA* low versus high expression in TCGA data plotted using TIMER (<http://timer.cistrome.org/>). **B**, Correlation of *INHBA* expression with melanoma disease stage. **C**, Kaplan-Meier survival analysis of YUMM3.3-Ctrl and - β A tumor-bearing mice treated with ICB therapy. Mice were considered dead when the tumor reached volume >1 cm³ (n = 11-12 per group). Curves were compared using the Log-rank (Mantel-Cox) test.

Supplementary Figure 9. Gating strategy for a 16-color flow cytometry antibody panel used for TILs profiling

Supplementary Figure 10. Gating strategy used in Fig. 2 and S2

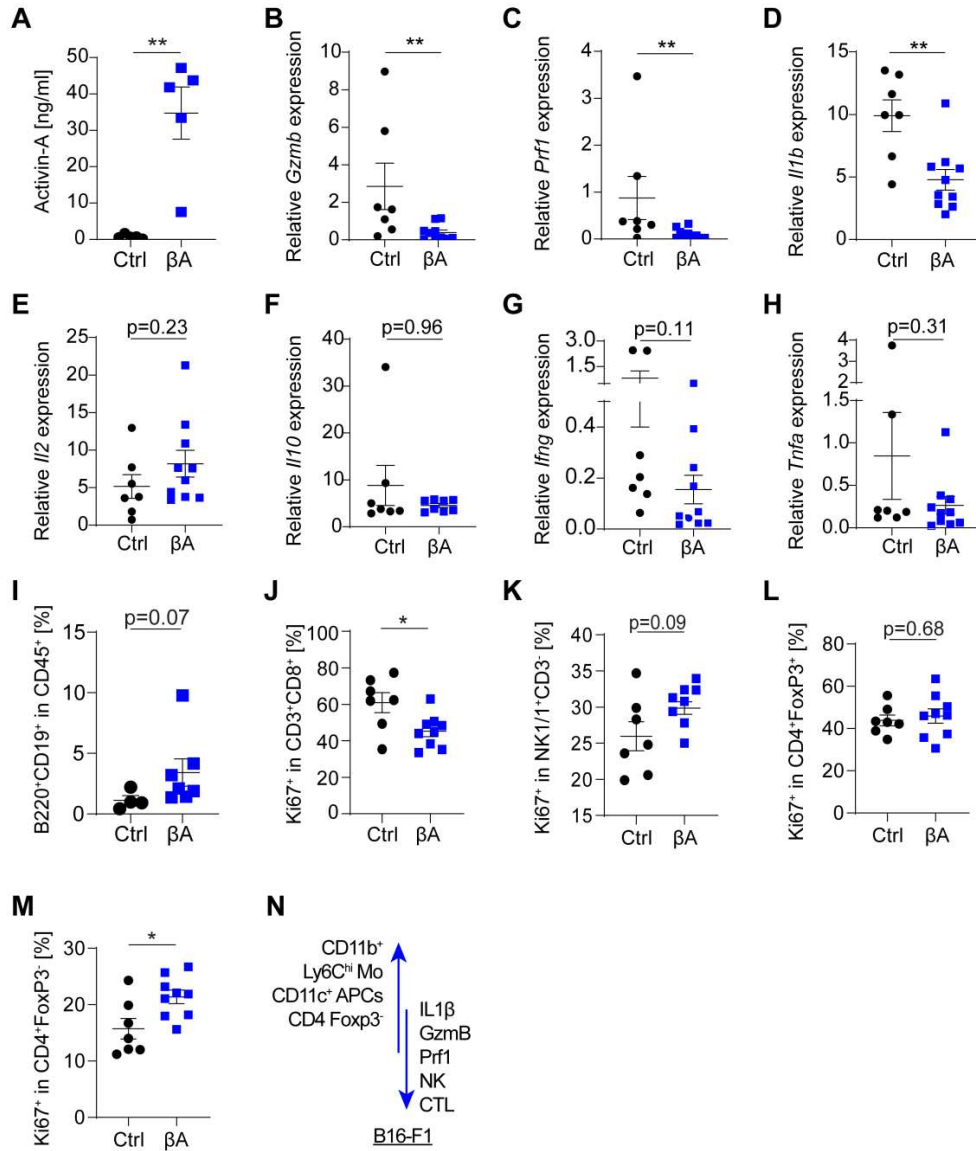
A B, Analyses of (A) OVA-specific T cells in tumors and (B) SIINFEKL presentation by APCs in tumors and LNs.

Supplementary Figure 11. Gating strategy used for ATCT analyses in Fig. 3 and S3

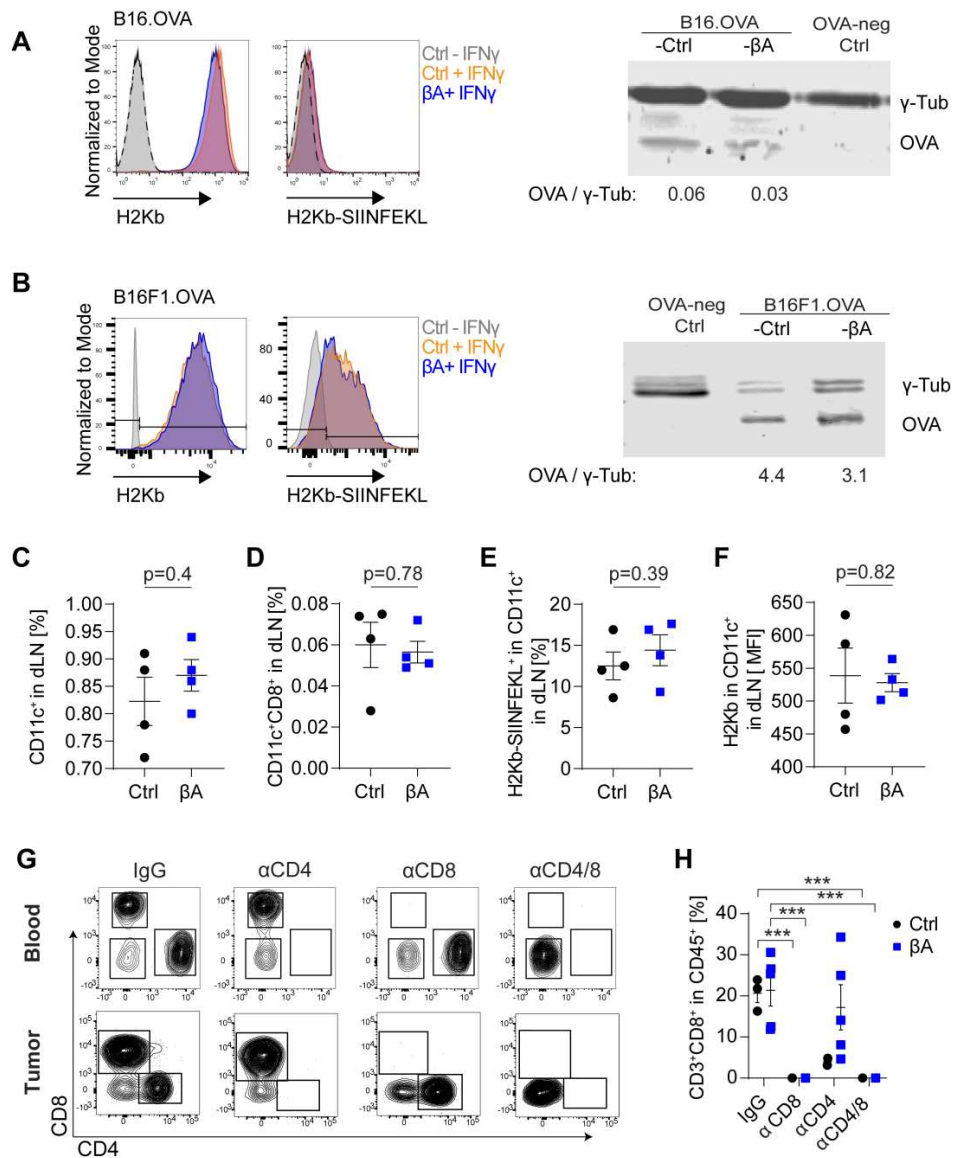
A B, Analyses of OT-I cells after the ATCT in (A) tumors and (B) LNs

Supplementary Figure 12. Gating strategy used in Fig. 5 and S7 to analyze CXCL9 expression in tumors

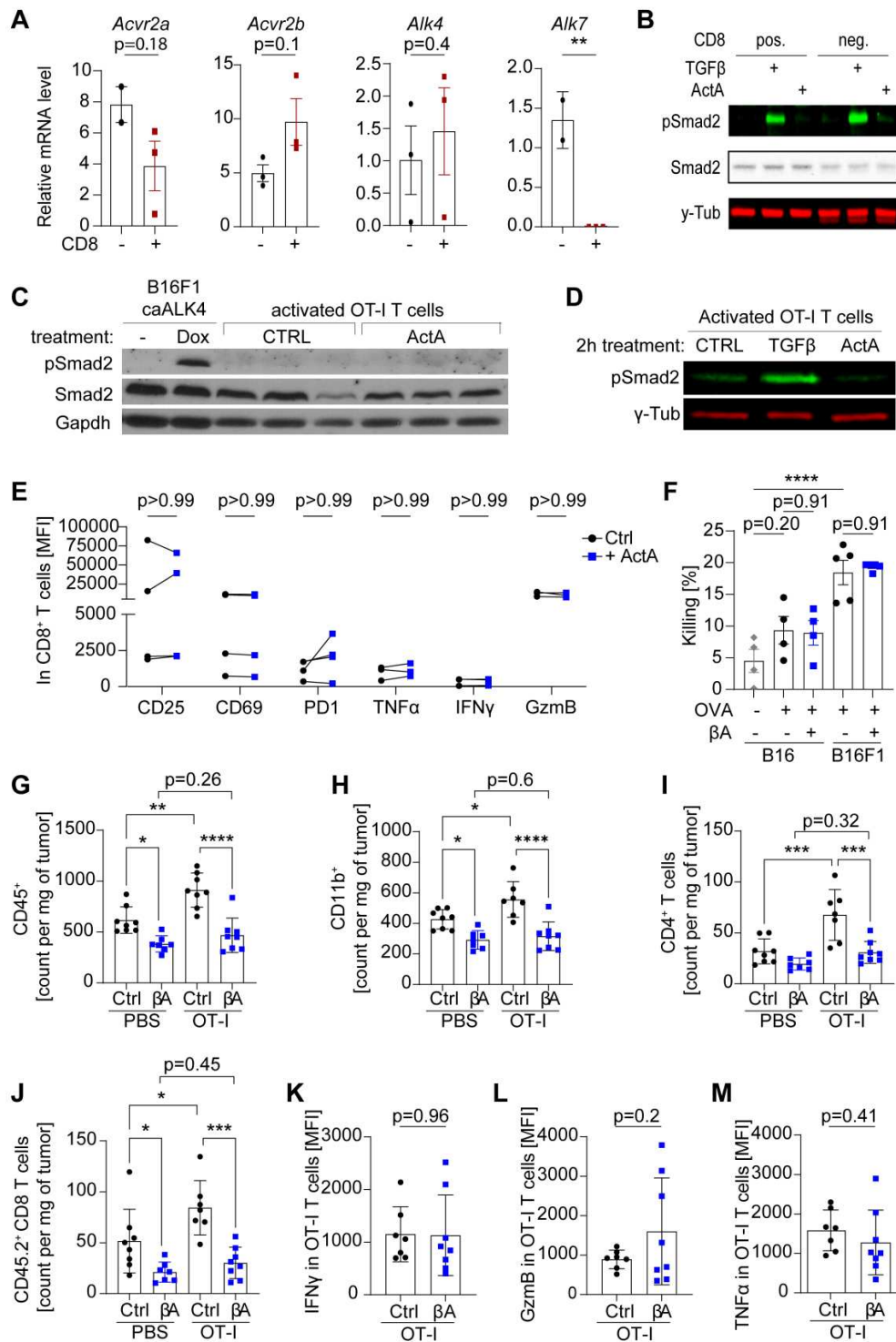
Supplementary Figure 1



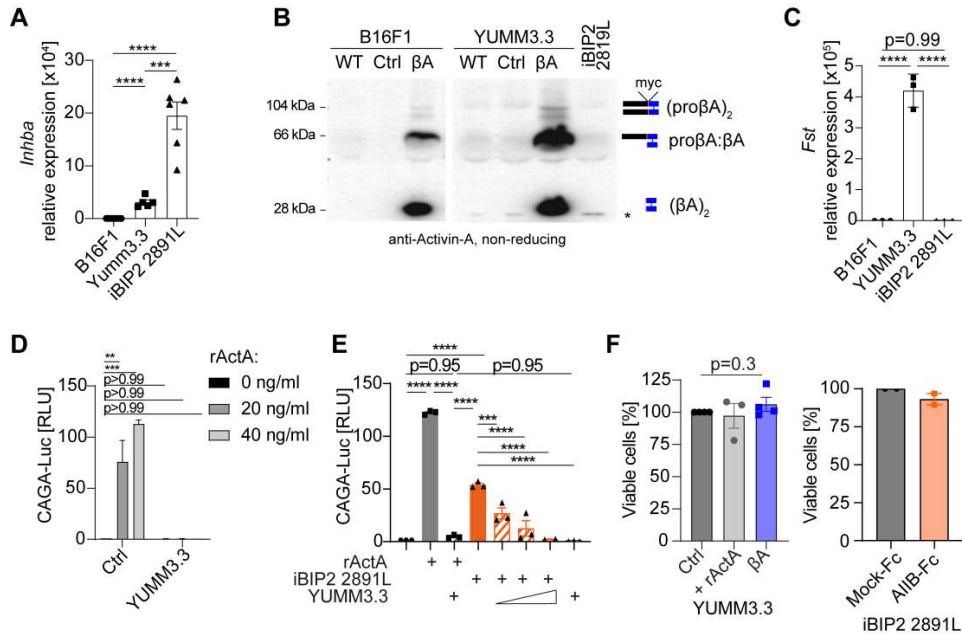
Supplementary Figure 2



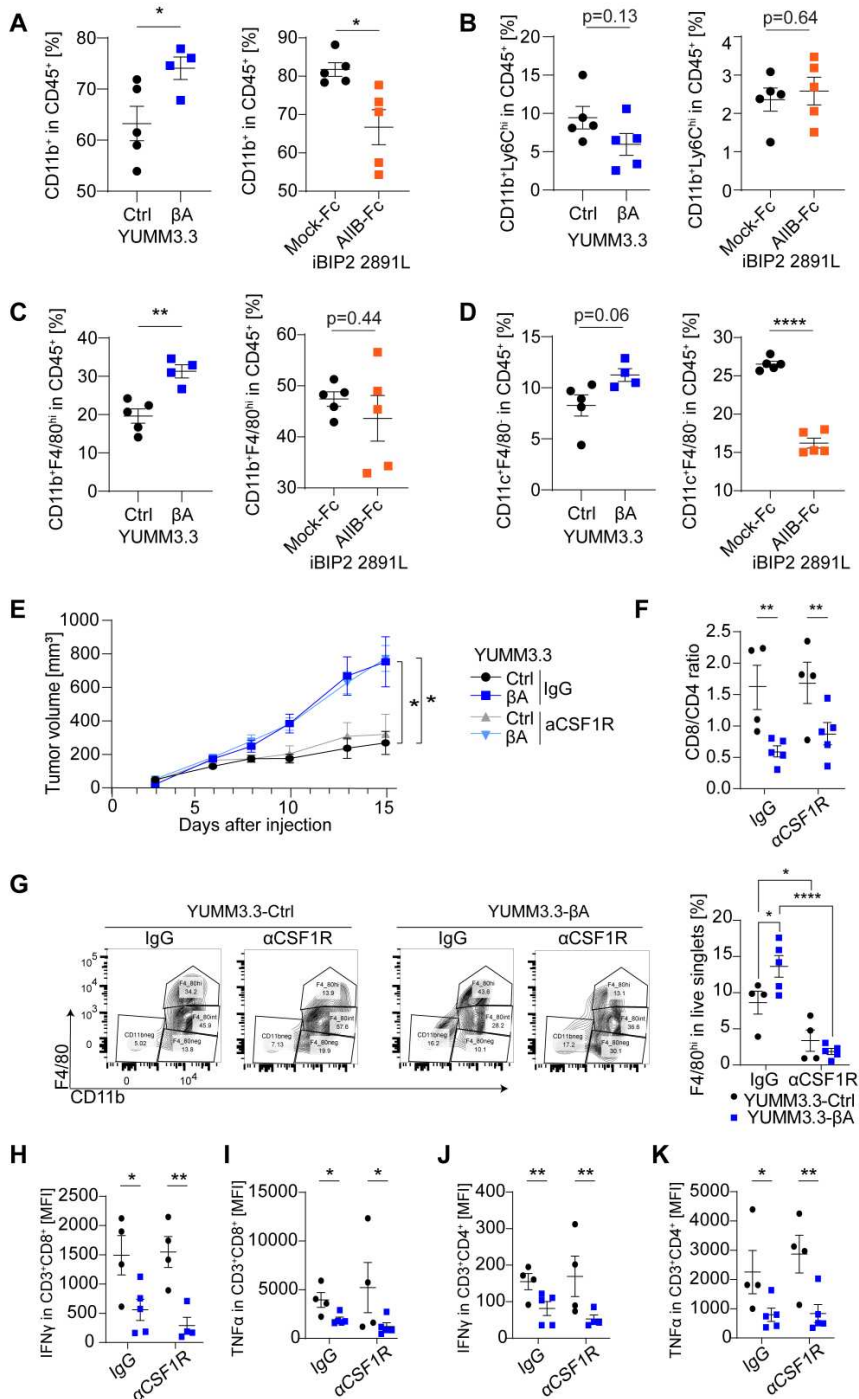
Supplementary Figure 3



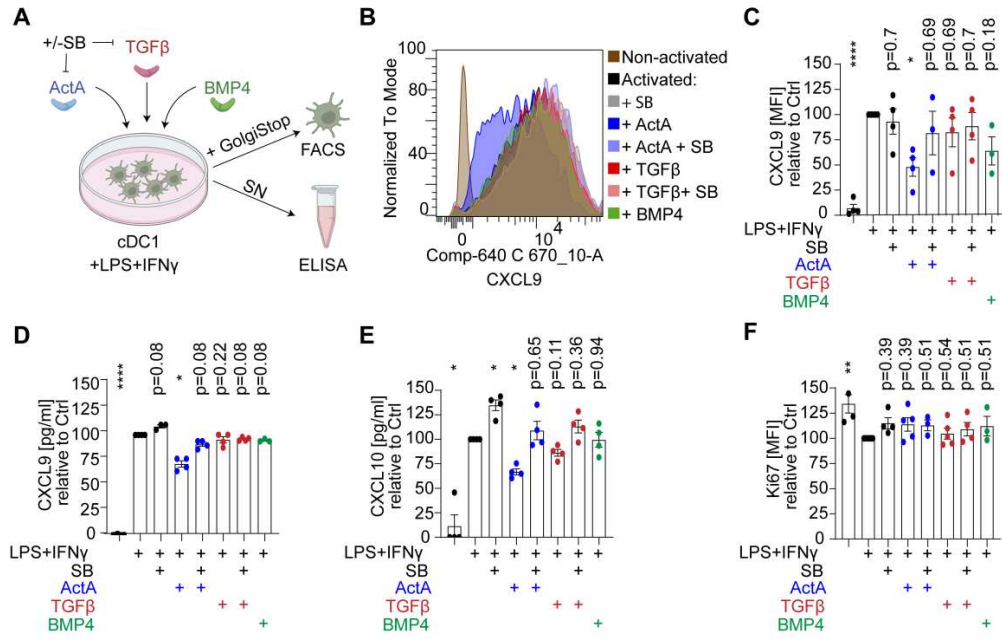
Supplementary Figure 4



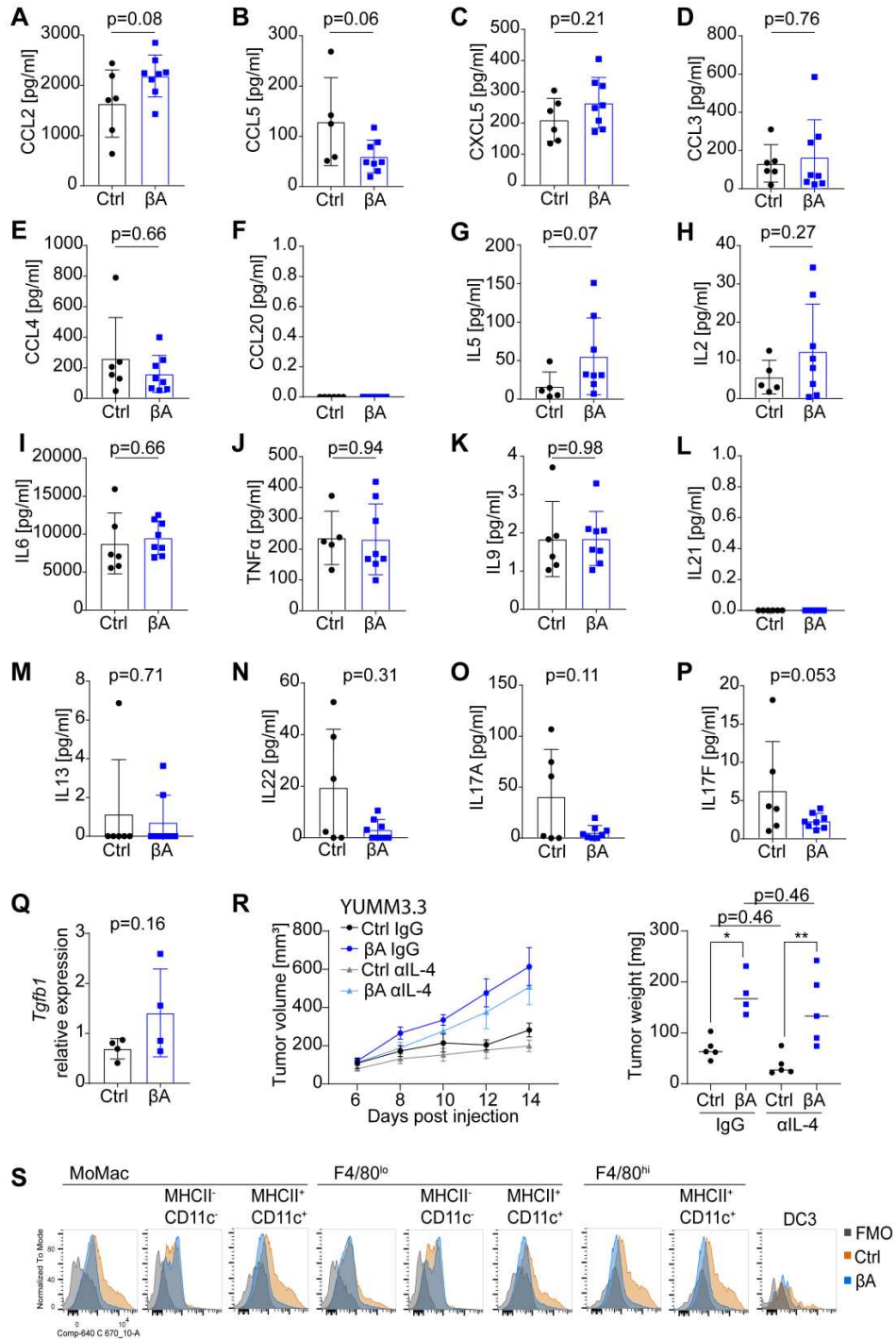
Supplementary Figure 5



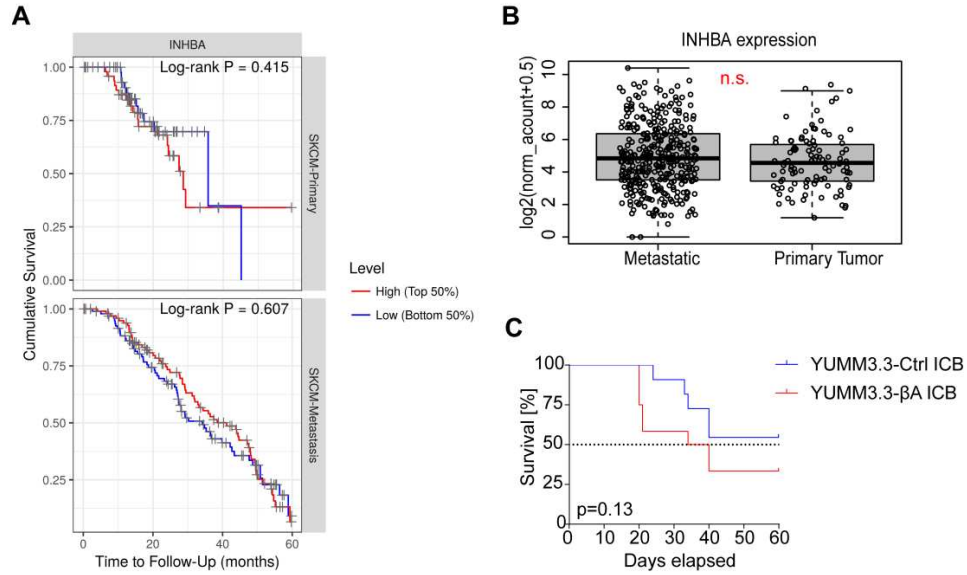
Supplementary Figure 6



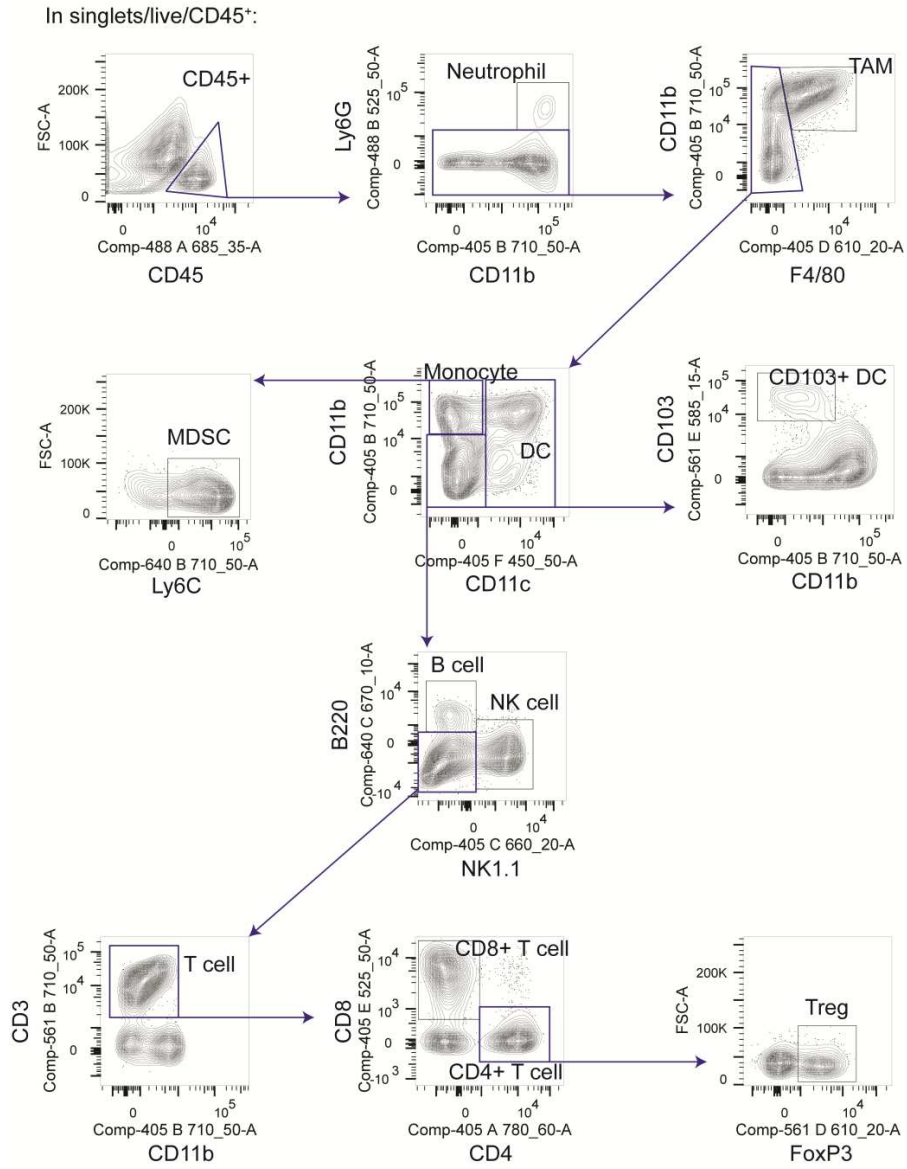
Supplementary Figure 7



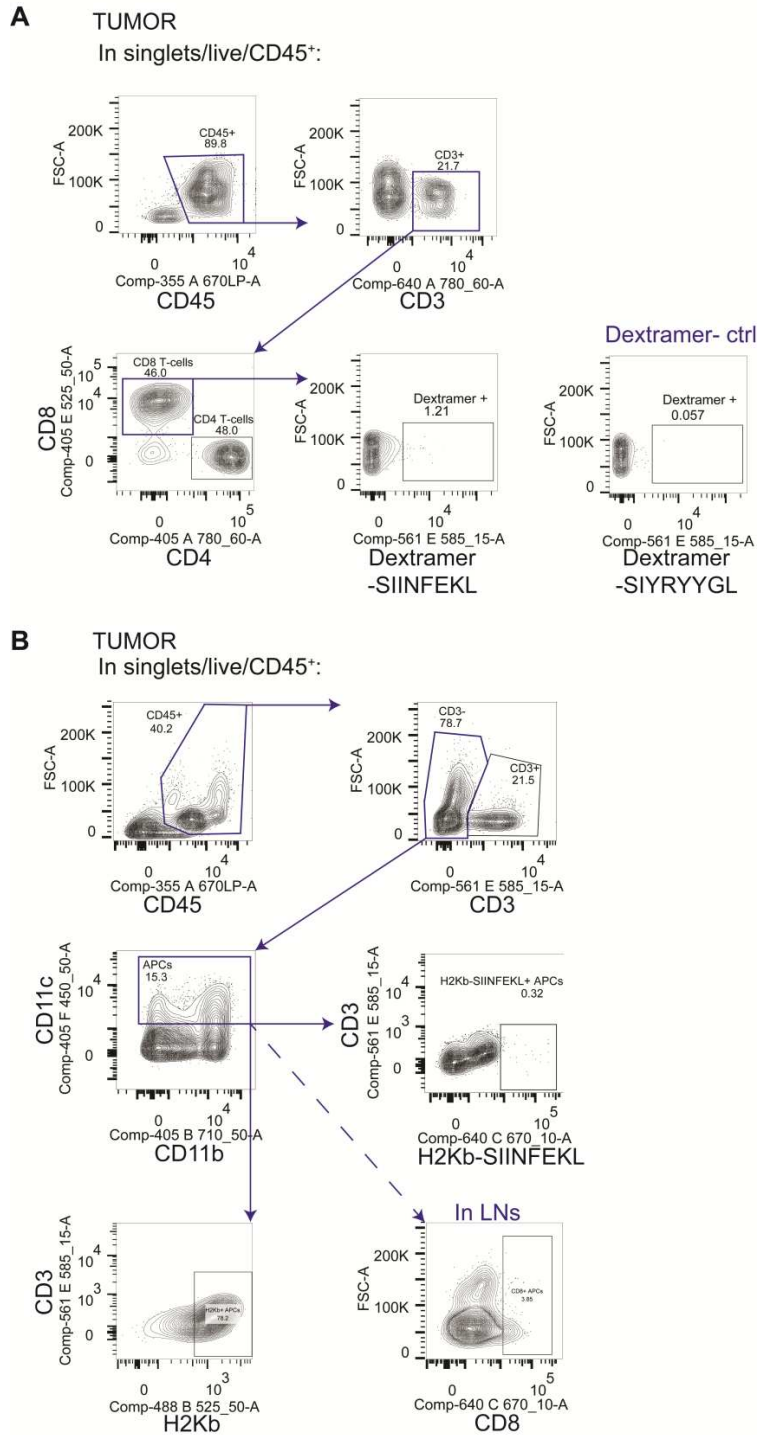
Supplementary Figure 8



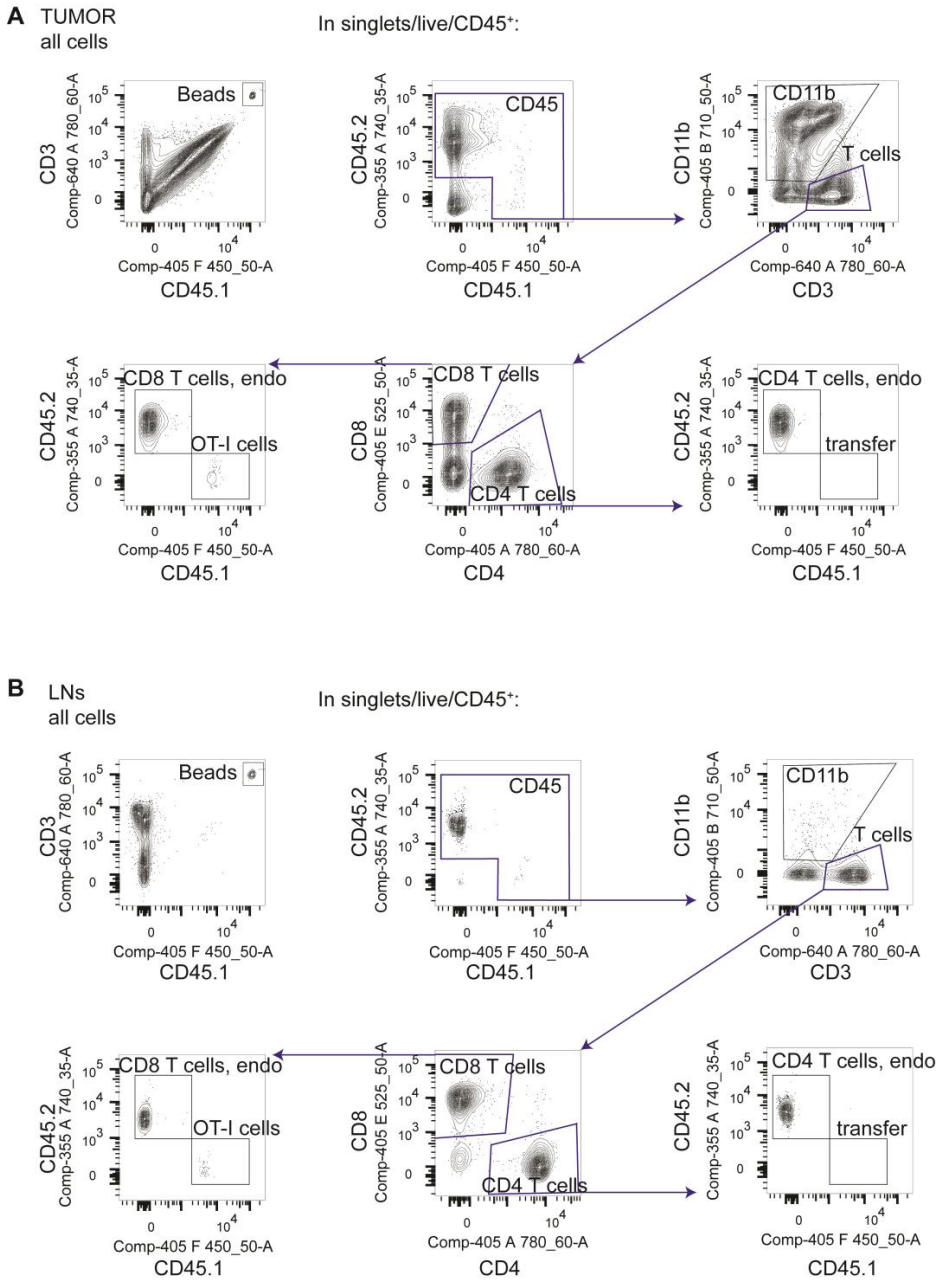
Supplementary Figure 9



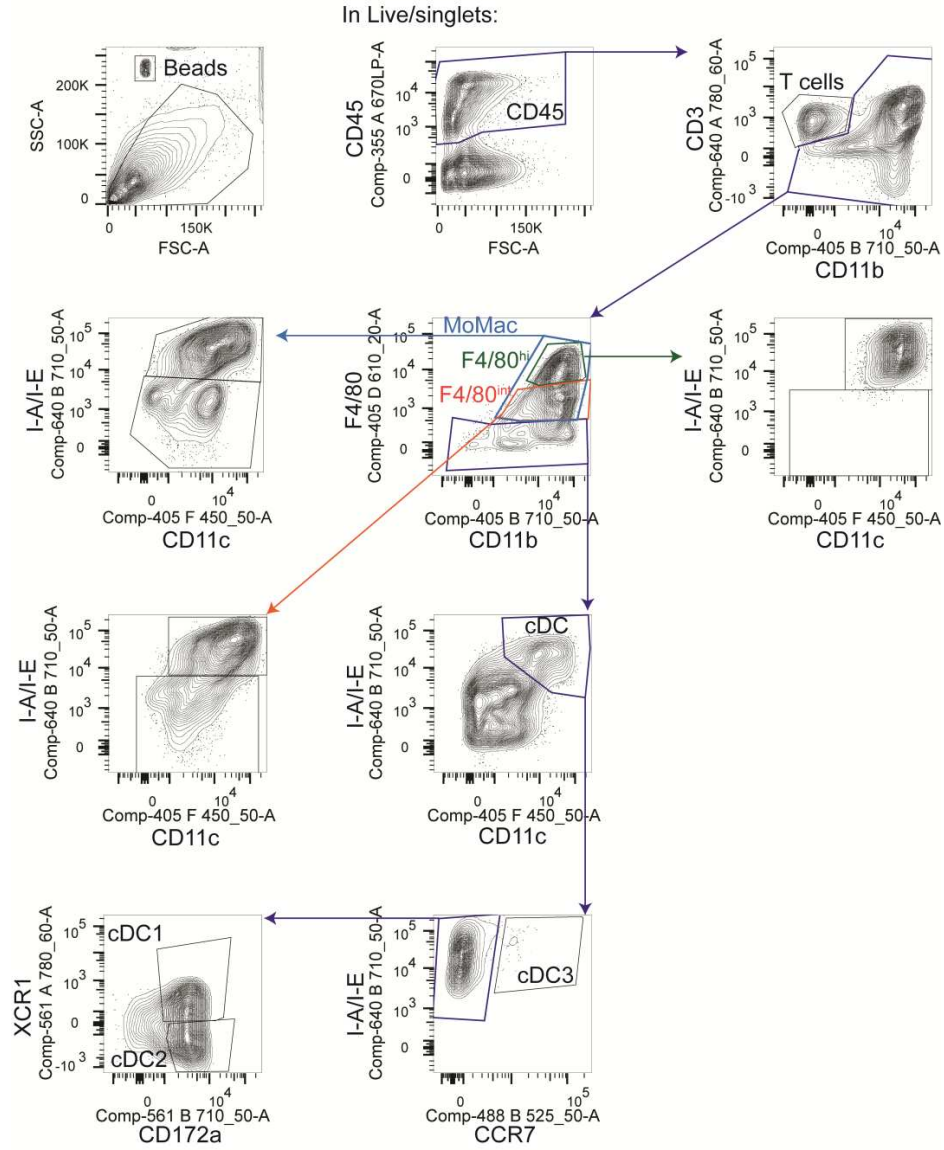
Supplementary Figure 10



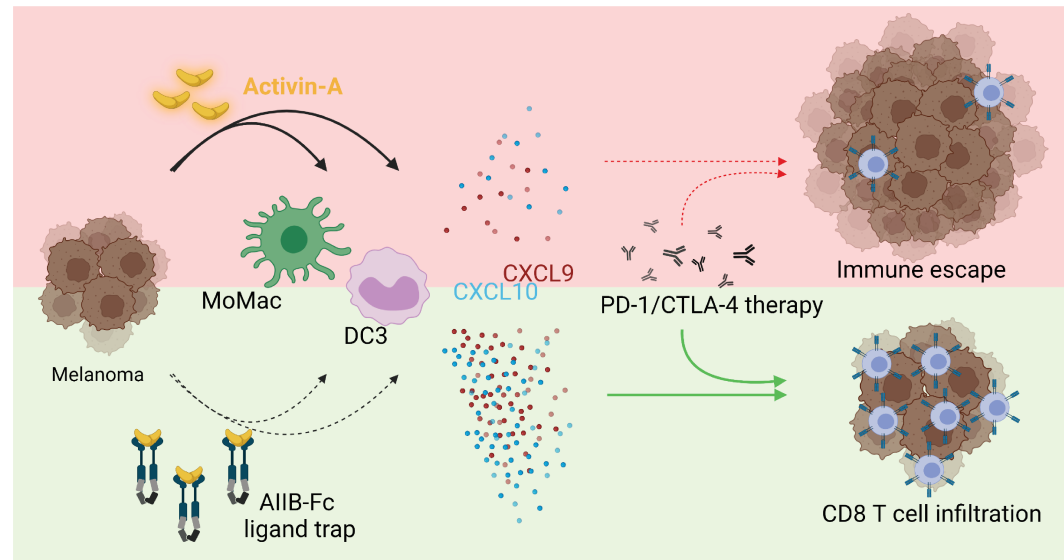
Supplementary Figure 11



Supplementary Figure 12



Activin-A impairs CD8 T cell-mediated immunity and immune checkpoint therapy response in melanoma



Authors

Katarina Pinjusic, Olivier A. Dubey, Olga Egorova, Sina Nassiri, Etienne Meylan, Julien Faget, and Daniel B. Constan

Correspondence

daniel.constam@epfl.ch

In Brief

Activin-A promotes immunotherapy resistance and tumor immune evasion by indirectly inhibiting CTL accumulation and function. Thus, Activin-A inhibition holds promise to boost anti-tumor immunity and immunotherapy.